



## Photoresponsive hydrogel-based soft robot: A review

Jingang Jiang<sup>a,\*</sup>, Shuainan Xu<sup>a</sup>, Hongyuan Ma<sup>a,b</sup>, Changpeng Li<sup>a</sup>, Zhiyuan Huang<sup>c</sup>

<sup>a</sup> Key Laboratory of Advanced Manufacturing and Intelligent Technology, Ministry of Education, Harbin University of Science and Technology, Harbin, 150080, Heilongjiang, PR China

<sup>b</sup> Harbin Branch of Taili Communication Technology Limited, China Electronics Technology Group Corporation, Harbin, 150080, Heilongjiang, PR China

<sup>c</sup> State Key Laboratory of Robotics and System, Harbin Institute of Technology, Harbin, 150001, Heilongjiang, PR China



### ARTICLE INFO

#### Keywords:

Photoresponsive hydrogels  
Response mechanisms  
Structural forms  
Soft robots  
Actuators  
Citespace

### ABSTRACT

Soft robots have received a lot of attention because of their great human-robot interaction and environmental adaptability. Most soft robots are currently limited in their applications due to wired drives. Photoresponsive soft robotics is one of the most effective ways to promote wireless soft drives. Among the many soft robotics materials, photoresponsive hydrogels have received a lot of attention due to their good biocompatibility, ductility, and excellent photoresponse properties. This paper visualizes and analyzes the research hotspots in the field of hydrogels using the literature analysis tool Citespace, demonstrating that photoresponsive hydrogel technology is currently a key research direction. Therefore, this paper summarizes the current state of research on photoresponsive hydrogels in terms of photochemical and photothermal response mechanisms. The progress of the application of photoresponsive hydrogels in soft robots is highlighted based on bilayer, gradient, orientation, and patterned structures. Finally, the main factors influencing its application at this stage are discussed, including the development directions and insights. Advancement in photoresponsive hydrogel technology is crucial for its application in the field of soft robotics. The advantages and disadvantages of different preparation methods and structures should be considered in different application scenarios to select the best design scheme.

### 1. Introduction

Traditional robots have been applied in medical, scientific, industrial, and military fields and have helped people live more productive lives. The majority of these robots are made up of rigid motion sub-connections made of rigid materials that can only work in structured environments and have poor flexibility, adaptability, and safety. In addition, soft robots have far more freedom and can operate in unstructured environments. Therefore, they can solve problems in a much safer manner [25]. Smart responsive materials are becoming increasingly popular as soft robotics advances. Smart materials have a wide range of applications in soft robotics [4,5] due to their bio-affinity, light weight [1], and flexible deformation [2,3].

Smart-responsive hydrogels are three-dimensional polymer networks that are physically or chemically cross-linked and have excellent biocompatibility, ductility, permeability, degradability, and stimulus adaptability [6,7]. To respond to a variety of external stimuli, smart responsive hydrogels interact with the polymer network and the external environment. Therefore, its use as an ideal material for soft robots can provide them with additional capabilities due to the material's unique

properties. When stimulated by temperature, pH, an electric or magnetic field, light, enzymes, or ion concentration, smart responsive hydrogels change their own physical or chemical properties. They have promising applications in sensors [8], tissue engineering scaffolds [9], microfluidic valves [10], bionic devices [11–13], medical carriers [14–16], and soft robotics [17] due to their tunable chemical structure and physical properties and rich stimulation sources. Photoresponsive hydrogels provide intelligent responsiveness through light stimulation without direct physical contact with external factors. The light allows for remote manipulation of the robot without the use of any additional reagents. Processes triggered by light can also be paused and resumed. Furthermore, the light parameters (intensity, wavelength, and light duration) can be adjusted to precisely control the degree of light response. Photoresponsive hydrogels, with proper design, can acquire photo-deformation and perform a variety of complex movements such as stretching, bending, crawling, and rotating. Lee [18], Liu [19], and others have recently reviewed hydrogel soft robots and various hydrogel applications. However, a comprehensive overview of photoresponsive hydrogel soft robots is still lacking.

This paper reviews current research on various response mechanisms,

\* Corresponding author.

E-mail address: [jiangjingang@hrbust.edu.cn](mailto:jiangjingang@hrbust.edu.cn) (J. Jiang).

<https://doi.org/10.1016/j.mtbio.2023.100657>

Received 15 February 2023; Received in revised form 13 April 2023; Accepted 3 May 2023

Available online 10 May 2023

2590-0064/© 2023 Published by Elsevier Ltd. This is an open access article under the CC BY-NC-ND license (<http://creativecommons.org/licenses/by-nc-nd/4.0/>).

structural forms, and applications of photoresponsive hydrogels in soft robots. The second section of this paper utilizes Citespace to analyze current literature in order to identify hot areas and the main directions of current hydrogel research. Section 3 examines the properties of the various response mechanisms, including photoisomerization, photo(de)crosslinking, and photothermal types. Section 4 reviews application advancements in soft robots based on bilayer, gradient, oriented, and patterned structures. Section 5 discusses the main issues affecting the application of photoresponsive hydrogels, solutions to these problems, and future directions. Section 6 provides a summary of the topics covered.

## 2. Analysis of research hotspots based on citespace

### 2.1. Citespace

Bibliometrics is a quantitative research method based on mathematical and statistical techniques to assess the external characteristics of scientific literature and predict current and future trends in scientific and technical research. Citespace (Version 6.2.R2, Drexel University, Philadelphia, PA, USA) was chosen as a tool for literature analysis in this paper. The software generates visual graphs that assist researchers in gaining insight into literature connections and citations, revealing intersections and trends between fields. And provide a scientific basis and reference for researchers and policymakers to support their decision making and planning.

### 2.2. Date sources

In this paper, we searched the Web of Science Core Collection for data from 2004 to 2023 using "photoresponsive hydrogel\*" as keywords, providing 398 documents. The Citespace visualization analysis software was used to conduct a qualitative analysis of the research on photoresponsive hydrogel, and the research was summarized. Identify current research hotspots and key technologies in the field of photoresponsive hydrogels.

### 2.3. Date analysis

In this paper, we employed the "Keyword" co-occurrence analysis

function in Citespace software to construct a keywords co-occurrence map for exploring the research hotspots and trends in the field of photoresponsive hydrogels. Fig. 1 illustrates the co-occurrence network among 330 nodes and 617 keywords. Each node denotes a keyword, and the size of the node circle reflects the frequency of the keyword in the graph, with key nodes having centrality greater than 0.1. Table 1 presents the top ten most frequently occurring keywords, together with their importance and year of occurrence. The greater the breadth and frequency of research, the more likely it is to become a research hotspot in the keyword co-occurrence network. The greater the centrality value, the more central the keyword is in the overall cooccurrence network. A node with high frequency but low centrality implies that the node, while frequent, does not occupy a central position. As shown in Table 1, photoresponsive hydrogel technology represents a current hot topic in the field of hydrogel applications. In addition, Fig. 2 shows an explosive citation trend for keywords related to photoresponsive hydrogels, indicating that these keywords represent the current hotspots and trends in hydrogel research, thereby validating the practical significance of this study.

## 3. Response mechanisms

Photoresponsive hydrogels have piqued the interest of a wide range of researchers as a non-contact stimulus with benefits such as remote control and programmed control. Furthermore, under NIR-UV light conditions, photoresponsive hydrogels undergo physical or chemical changes in the hydrogel network, resulting in varying degrees of swelling

**Table 1**  
Keywords co-occurrence count, centrality and year.

keyword	count	centrality	Initial year of the literature
Hydrogels	100	0.15	2007
Drug delivery	52	0.26	2004
Polymers	43	0.12	2006
Release	43	0.07	2010
Nanoparticles	36	0.06	2011
Light	34	0.12	2008
Behavior	30	0.17	2007
Photodegradable hydrogel	26	0.10	2010
Photoresponsive hydrogel	20	0.11	2015

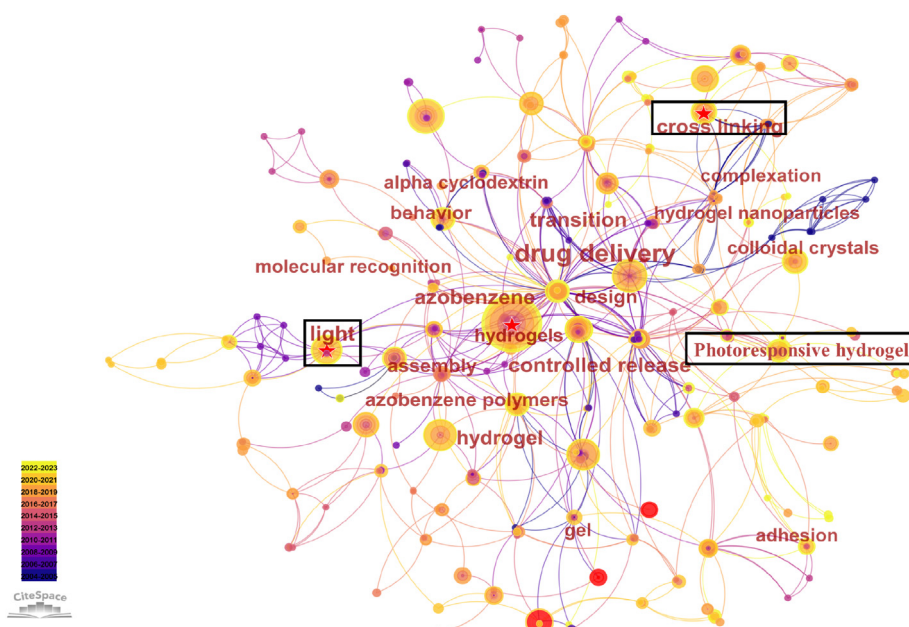


**Fig. 1.** Keywords co-occurrence network map of photoresponsive hydrogel.

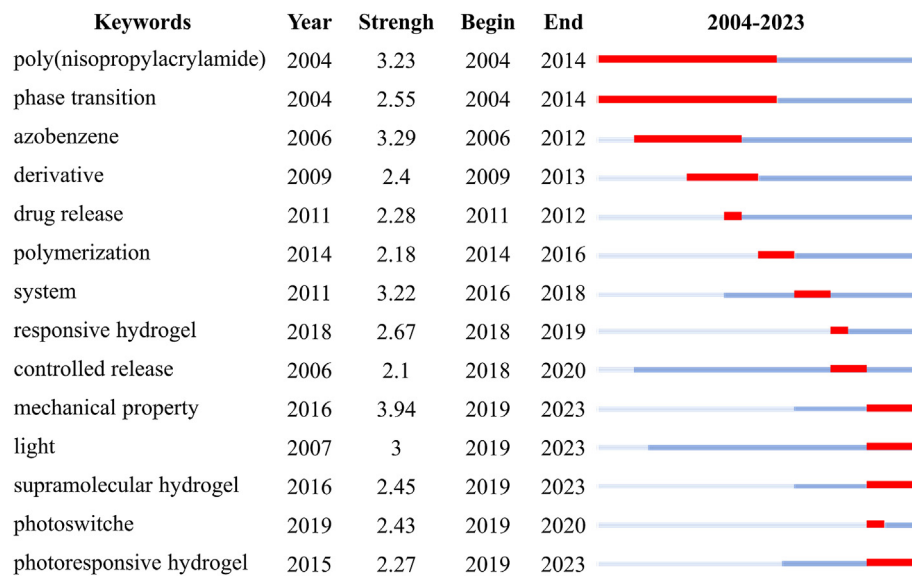


Fig. 2. Keywords with the strongest citation bursts.

or shrinkage. Photoresponsiveness is primarily photochemical and photothermal in nature. The photochemical effect is based on photoreactions of photosensitive groups, such as photoisomerization and photo(de)crosslinking; the photothermal effect is the use of photothermal conversion and thus volume transformation of the hydrogel, which we will discuss in more detail later (Table 2: Properties of photoresponsive hydrogels with different response mechanisms).

### 3.1. Photoisomerization

Photoisomerization is the transformation of a hydrogel from a photo-unstable to a photo-stable state as a result of light irradiation or by changing the hydrogel from a ground state to an excited state using a

triplet state photosensitizer. Many molecules, such as azobenzene and its derivatives or spiropyran and its derivatives, can cause photoisomerization [20–22,41]. When this class of groups is irradiated with light of corresponding wavelengths, electrons within the group leap, molecular orbitals enter the excited state, and the excited molecule induces reversible isomerization of the group via inter and intramolecular potential energy transfer. For example, the *cis-trans* transition of the azo phenyl group and the anatase structure's ring closure and ring opening within the spiropyran group (Fig. 3a) [23,24].

The isomerization of the azobenzene molecule can be viewed as a typical *cis-trans* isomerization process. The polar groups in the *cis*-isomer, such as the azo bond, are drawn together in the presence of light, increasing the polarity of the molecule. In contrast, the polar groups in

**Table 2**  
Properties of photoresponsive hydrogels with different response mechanisms.

Article Information	Composition of hydrogels	Mechanisms of photoreactions	Applications	Advantages	disadvantages
Wang et al.(2019) [27]	Azobenzene, $\alpha$ -CD	Photoisomerization	Optoelectronic devices	1.Reversible 2.High biocompatibility 3.Rapid response	1.Additional light source required 2.Insufficient accuracy
Bian et al.(2017) [125]	Azo-PDMAEMA PAA, $\beta$ -CD	Photoisomerization	Delivery applications		
Satoh et al.(2011) [126]	Sp, NIPAAm	Photoisomerization	Biomedical field Delivery applications	1.Reversible 2.High biocompatibility 3.Suitable for use in the biomedical field	1.Slow response
Chen et al.(2017) [127]	SP, Dox N-bis(acryloyl) cystamine	Photoisomerization	Cell imaging		
Cai et al.(2019)[38]	HA, O-nitrobenzyl alcohol	Photo(de)crosslinking	Cell culture	1.Reversible 2.Fast crosslinking	1.Durability decreases with time and repeated application 2. Requires photosensitizer
Lunzer et al.(2018) [128]	O-nitrobenzyl, PEG, HA	Photo(de)crosslinking	Cell culture		
Yang et al.(2017) [129]	AzoAAM, $\beta$ -CD	Photo(de)crosslinking	Sensors	1.Reversible 2.Self-healing	
Cao et al.(2022) [130]	Fe <sub>3</sub> O <sub>4</sub> , P(NIPAM-AM)	Photothermal	Actuators Biomedical devices	1.Large bending angle(107.8°) 2.Reversible 3.Magnetic response	1.Prone to aggregation, reducing photothermal conversion efficiency
Lee et al.(2015)[124]	MNP, PNIPAM	Photothermal	Actuators	1.Rapid response 2.Reversible 3.Constant curvature variation ( $k \sim 7.5 \text{ mm}^{-1}$ )	
Shao et al.(2018) [131]	BP, PDLLA-PEG-PDLLA	Photothermal	Photothermal therapy (PTT)	1. High biocompatibility and biodegradability 2. Suitable for biomedical applications 3. High photothermal antibacterial properties (>99.5% killing efficiency)	1.Urface modification is required to improve its stability

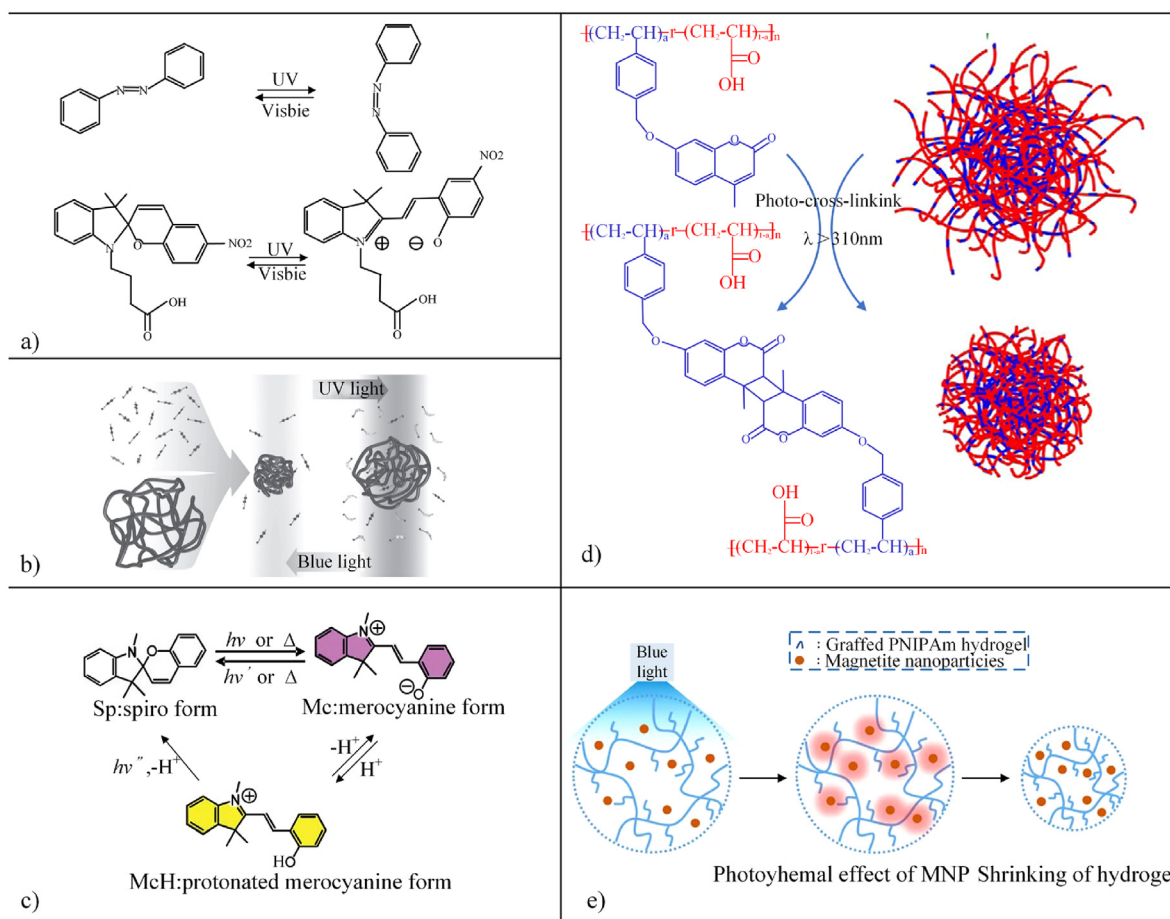


**Fig. 3.** a) Photoisomerization of Azobenzene [20] and Spiropyran. Reproduced with permission. Copyright 2011, Elsevier. b) Microgel particles converted to *cis*-structure under UV light and *trans*-structure under blue light [29]. Reproduced with permission. Copyright 2012, Wiley-VCH. c) Chemical structures and isomerizations of spiropyrans [31]. Reproduced with permission. Copyright 2011, Royal Society of Chemistry. d) Schematic illustration of photo-crosslinking reaction among PVMAA and the structures of the PVMAA micelles and those photo-crosslinked [37]. Reproduced with permission. Copyright 2014, American Chemical Society. e) Volume deformation of MNPs-containing hydrogels under blue light irradiation [42]. Reproduced with permission. Copyright 2015, Springer Nature. (For interpretation of the references to color in this figure legend, the reader is referred to the Web version of this article.)

the *trans*-isomer are dispersed, decreasing the polarity of the molecule. The isomerization of an azobenzene molecule can result in modifications to its morphology and structure on a macroscopic level.  $\pi$ -electrons from the azo bond are added to the  $\pi$ -electron conjugated system on the benzene ring, increasing the conjugation length of the entire molecule, when a phenyl group in an azobenzene molecule forms a conjugated system with an adjacent nitrogen atom. This change can lead to a shift in the azobenzene molecule from a linear to a cyclic structure. *Trans-cis* photoisomerization [32] under UV irradiation causes an increase in the dipole moment [33], which causes the monomolecular film to swell and the *cis*-azobenzene to have a higher affinity for the water surface. In contrast, it returns to the *trans* conformation when exposed to visible light (Fig. 3b) [29]. Azobenzene groups have been used to make photo-sensitive hydrogels with different modifications, such as polymers [26], cyclodextrins [27], and peptides [28].

Spirobenzopyrans can change their conformation in response to light, changes in temperature, and the presence of additional protons. Although spirobenzopyrans themselves are not water-soluble, they can be used in aqueous systems when combined with water-soluble polymers. Most chromophores in acidic aqueous solutions exist as protonated open-loop isomers (protonated anthocyanine form: McH). When exposed to visible light, McH is effectively isomerized into a closed-loop isomer (spiro form: Sp) (Fig. 3c). Sp spontaneously transforms into the thermodynamically stable McH when the irradiation stops. McH is an ion, resulting in it being a more hydrophilic molecule than Sp, which is a

highly hydrophobic molecule. Therefore, p(NIPAAm) chains in spirochroman-conjugated p(NIPAAm) (p(Sp-NIPAAm)) are induced to dehydration or hydration, respectively, by Sp and McH [31]. The p(NIPAAm) gel's size changes depending on how much of the p(NIPAAm) chain is dehydrated or hydrated. Since the volume change is reversible, p(Sp-NIPAAm) gels can therefore swell in acidic aqueous solutions in the dark and shrink quickly when exposed to visible light at room temperature [30].

### 3.2. Photo(de)crosslinking

Photo-crosslinking is the photo-driven generation of polymer branches based on one of two photopolymerization mechanisms [34]: Chain growth radical propagation reactions or step growth radical propagation reactions. Both can be controlled by the addition of a photoinitiator to the reaction system [35]. The chain growth radical growth reaction occurs when a monomer molecule forms a radical in the presence of a photoinitiator. The radical is continuously transferred within the molecule, facilitating the bonding reaction that forms polymer branches between the molecules. The step-growth radical growth reaction involves the photoinitiator exciting electrons upon UV light absorption. The electrons will form covalent bonds with the monomer molecules, resulting in the formation of polymer branches. In contrast to chain growth, which consists of repeating single steps, step growth consists of two alternating steps. For example, the thiol-ene reaction alternates between thiyl radical propagation across the

ene functional group and carbon-centered radical abstraction of a hydrogen radical from thiol. Step growth reactions are thought to be less susceptible to oxygen inhibition and more controllable and biocompatible than chain growth reactions. Photodimerization also provides reversible cross-linking points for hydrogels. Coumarin, cinnamic acid, anthracene, and poly are common photodimerization groups. Lin et al. [36] created hydrogels by phototransforming sulfhydryl groups via sulfhydryl-Michael addition reactions using macrocyclic coumarin-protected photo-transformed molecules. In the same year, Liu et al. developed Poly(7-(4-vinylbenzyloxy)-4-methylcoumarin-co-acrylic acid) (PVMAA) hydrogels. Chemical cross-linking occurs within the hydrogel when exposed to light at wavelengths greater than 310 nm, resulting in a cross-linked network structure and a rapid change in particle size (Fig. 3d) [37]. Photodimerization groups can be used to initiate gelation and control the gel-sol transformation.

Photodegradation is the opposite process of photocrosslinking. Photodegradation hydrogels typically have photodegradation groups along the polymer's main or side chains. These groups undergo chain-breaking reactions, which cause the hydrogel network to disintegrate. Photosensitive groups include *o*-nitrobenzyl and its derivatives. The photodegradation reaction of *O*-nitrobenzyl is usually irreversible and causes varying degrees of disruption to the polymer network [38]. Because of their biocompatibility, fast cleavage rate, red-shift absorption, and two-photon induction, coumarin derivatives are commonly used as alternatives to *O*-nitrobenzyl derivatives [39]. Various coumarin derivative modifications have been developed to increase their absorption into biologically relevant ranges.

### 3.3. Photothermal

#### 3.3.1. Photothermal agents

Photothermal hydrogels are mainly temperature-sensitive hydrogels with gold nanorods, carbon nanotubes, graphene, Go nanosheets, and magnetite nanoparticles [43,44]. When light strikes the surface of a photothermal agent, it causes its internal electrons to vibrate and excite, causing the photothermal agent to absorb light energy and convert it into heat energy. Different photothermal agents have different optical properties and energy band structures, their light absorption and conversion mechanisms differ.

Metal nanoparticles' [40] unique surface plasmon resonance effect allows absorbed light energy to be efficiently focused on a localized area near the nanoparticles and generate high temperatures. Furthermore, metal nanoparticles have a high thermal conductivity, allowing them to rapidly transfer heat to their surroundings, resulting in efficient photothermal conversion. The most common plasma metals used in photothermal applications are gold (Au) [45] and silver (Ag) [46] metal nanoparticles. Metal nanoparticles are poorly compatible with hydrogels due to their proclivity to oxidize, forming agglomerates and precipitates in water. Graphene and its derivatives exhibit [69,70] good efficiency and stability in photothermal conversion due to their monolayer, two-dimensional structure and excellent optical properties. Graphene's photothermal conversion mechanism is primarily based on the absorption of light energy and its conversion to thermal energy. Its high thermal conductivity allows for the rapid transfer of thermal energy to the surrounding environment. When interacting with hydrogels, graphene displays excellent dispersion and stability. Carbon nanotubes [91] have a similar mechanism to graphene and are compatible with hydrogels. Carbon-based materials are gaining popularity in some applications, such as the biomedical field, due to their high biocompatibility and degradability.

MXene is a class of two-dimensional materials with high electrical conductivity and energy storage properties that can efficiently convert light energy to thermal energy [92,118]. The hydrogel's physical and chemical stability is ensured by the fact that it does not oxidize or degrade even after prolonged exposure to water. BN (boron nitride)

[121] is a two-dimensional material with photothermal conversion properties similar to MXene. They both have the advantage of controllable thickness and structure, allowing for the regulation of the hydrogel's thermal stability and thermal conductivity. MXene has an oxide functional group on its surface, making it hydrophilic. This makes MXene more easily interact with water molecules and form hydrogel complex systems than BN.

The compatibility of the photothermal agent with the hydrogel must be considered when creating photoresponsive hydrogels. To improve their compatibility with the hydrogel, different photothermal agents require different surface modifications or treatments. To achieve optimal photothermal conversion effects and special functionality, the selection of photothermal agents must be optimized for specific application scenarios and requirements.

#### 3.3.2. Photothermal conversion

The photothermal agent absorbs specific wavelengths of light and converts them into heat, increasing the internal temperature of the hydrogel. The volume phase transition temperature (VPTT) is the temperature of the sol-gel phase transition, which means that the hydrogel is in the sol state when it is below VPTT and in the gel state when it is above VPTT. The spatial structure of the hydrogel changes during this process, regulating its physical state. For example, when metal nanoparticles are exposed to light, they generate high temperatures, causing the hydrogel to gel. Conversely, they cool down and bring the hydrogel into solution.

Significant progress has been made in research aimed at hydrogel materials based on the VPTT principle. UV photopolymerized surface-modified Fe<sub>3</sub>O<sub>4</sub> nanoparticles were incorporated into poly(*N*-isopropylacrylamide-acrylamide) hydrogels to produce reversible photothermal deformation hydrogels, according to Cao et al. [47]. This reversible hydrogel can adjust its physical state in response to light intensity and frequency, allowing for precise control of its morphology. Lee et al. combined a comb hydrogel matrix with photothermal magnetite nanoparticles (MNP) dispersed in the matrix, allowing the hydrogel to change volume in 1 min (Fig. 3e) [42]. The results show that using comb-type hydrogel matrices with photothermal magnetite nanoparticles can improve the responsiveness and swelling rate of photo-responsive hydrogels, opening up a new avenue for the development of photothermal mechanical conversion materials. Jeon et al. adopted PNIPAM-BP with gold nanospheres as the active layer and a unique tapered optical fiber attached to the bilayer hydrogel driver. Green light is directed through the optical fiber to the PNIPAM-Au nanolayer, causing it to bend [48]. The optical fiber conduction control method provides more consistent and long-lasting control than traditional external light stimulation methods. Fiber optic conduction control allows for finer control of the target area by providing more precise light delivery and positioning, reducing interference from external environmental factors. In practical applications, the size and shape of the fiber optic conduction control equipment influence the location and size of the target area. Cost, equipment complexity, space constraints, and preparation size are all factors to consider when deciding whether it is appropriate for a specific application.

LCST hydrogels [122] are hydrogels with a lower critical solubility temperature. When the temperature falls below the LCST, the hydrogel loses solubility and undergoes a gel-sol phase transition [123]. Its molecular chains shrink inward, resulting in a decrease in gel volume when an LCST-based hydrogel is exposed to high temperatures (for example, at higher internal temperatures). This volume reduction causes pressure on the drug in the gel, allowing for faster drug release in biomedical applications. Hydrogels based on poly(methyl vinyl ether) have a stable photothermal response and are biocompatible. UV light or temperature changes can reversibly self-assemble and depolymerize them. Furthermore, YU et al. proposed a novel PTT system to address photothermal therapy (PTT) formulation [138], biodegradability, and delivery [124]. This system is made up of PDLLA-PEG-PDLLA thermosensitive gel and

black phosphorus (BP) nanosheets. The system has excellent near infrared (NIR) photothermal performance and high biocompatibility and biodegradability. Thus, it is utilised in post-operative cancer treatment.

#### 4. Structure and application of soft robot

Soft robots have attracted an increasing number of researchers in recent years due to their superior flexibility and biadaptability. The

unique properties of photoresponsive hydrogels expand the design possibilities for soft robots. Bilayer structures, gradient structures, oriented structures, and patterned structures are the most common anisotropic structures of photoresponsive hydrogels. Researchers have created a variety of soft robots based on the different structures, including soft grippers, crawling robots, walking robots, jumping robots, and swimming robots.

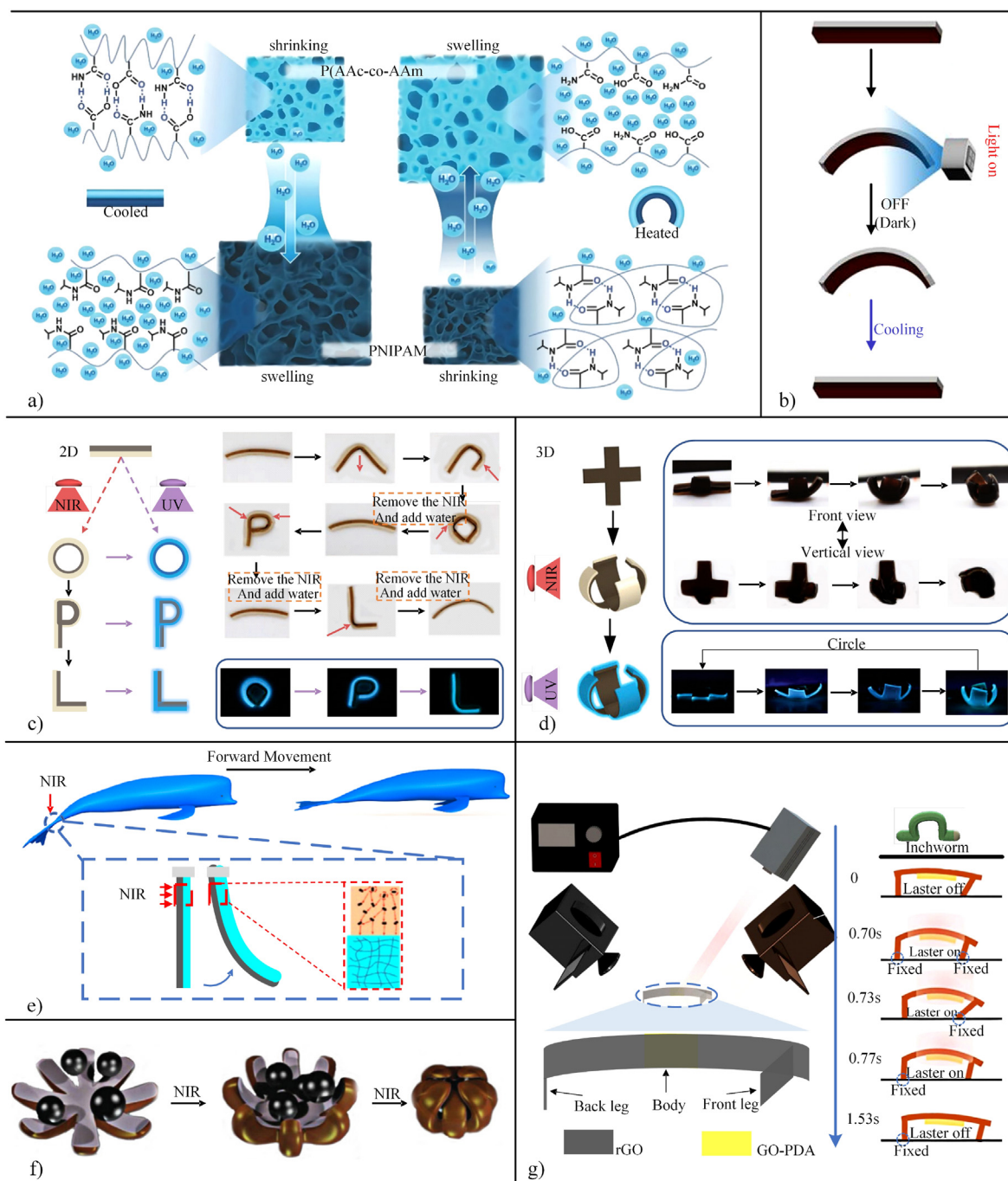


Fig. 4. a) Schematic diagram of bending of PNIPAM layer/P(AAc-co-AAm) layer [49]. Reproduced with permission. Copyright 2018, Royal Society of Chemistry. b) Schematic of the static bending motion of the bilayer actuator [54]. Reproduced with permission. Copyright 2016, American Chemical Society. c) The design and deformation of the 2D actuator [57]. d) The design and deformation of the 3D actuator [57]. Reproduced with permission. Copyright 2021, Wiley-VCH. e) Significant diagram of White Whale Software Robot Movement [64]. Reproduced with permission. Copyright 2019, American Chemical Society. f) Magnetic parcel micro transport robot [61]. Reproduced with permission. Copyright 2013, Wiley-VCH. g) One cycle locomotion of inchworm [63]. Reproduced with permission. Copyright 2019, IEEE.

#### 4.1. Bilayer structure

The bilayer structure [80], which consists of two hydrogels with different levels of water absorption and swelling, has been studied the most. One of the layers changes volume more than the other when exposed to external stimuli, causing the bilayer hydrogel to bend (Fig. 4a) [49], which results in more complex deformations. The characteristics of photoresponsive hydrogels with a double-layer structure are outlined in Table 3.

Bilayer structured hydrogels are produced via stepwise polymerization. During the preparation process, the monomer solution of the second layer penetrates slightly into the first layer, forming an interpenetrating network at the interface that serves as a junction layer connecting the two layers. By free radical polymerization of *N*-isopropylacrylamide (NIPAm) with AuNPs and AAm as photothermal conversion agents, Shi et al. successfully synthesized photoresponsive hydrogel actuators [53]. Since the acrylamide gel monomer can diffuse into the PNIPAM network to form an interpenetrating network and the AuNPs have a high photothermal conversion efficiency, an interpenetrating network can be formed. Therefore, the actuators possess exceptional bending properties. Zhao [50] designed a double layered nano composites hydrogel actuator containing nanofibrillar cellulose (NFC) and poly (*N*-isopropylacrylamide) clay using one-step in situ radical polymerization. The response time was decreased (31s–20s) by increasing the NFC content to increase the cross-link density of the bilayer hydrogel, increasing the anisotropic swelling difference, and decreasing the anisotropic de-swelling difference. Through stepwise in situ polymerization, Zhang et al. produced bilayer hydrogels containing GO-PNIPAM NC and PNIPAM NC gels [52]. Due to the high photothermal conversion efficiency of GO, the GO-PNIPAM NC layer's hydrogel warmed at a faster rate than the other layer, resulting in bending. In addition, increasing the GO concentration (strength is greatest at 3 mg/ml) can increase the number of hydrogen bonds in the PDMAA layer, thereby enhancing the hydrogel's mechanical strength and self-healing properties [51]. By combining magnetic nanoparticles with the photothermal effect, Yoon et al. designed a bilayer hydrogel brake consisting of poly(*N*-isopropylacrylamide)-graft-methylcellulose (PNIPAm-g-MC) as the active layer and polyacrylamide (PAAm) as the passive layer, which can be caused to shrink in volume by excessive cooling (Fig. 4b) [54]. In order to avoid the issue of rGO repacking in aqueous solution, photo-responsive poly(*N*-isopropylacrylamide) (PNIPAm/rGO) hydrogels were prepared by chemically reducing GO within the hydrogel matrix.

In addition, other functional hydrogels can be produced by incorporating hydrogel sheets into the stepwise polymerization process. Oxygen from the air bubbles on the surface of the Teflon plate gradually enters the solution during the polymerization and gelation processes using molds made of a Teflon plate and a glass plate. This reduces the polymerization efficiency and crosslink density as a result of the polymerization being slowed or inhibited. Adding GO nanosheets to form H-bonds with PNIPAM chains increased the crosslinking density, mechanical properties (by a factor of 9), and photothermal conversion efficiency [55]. Ma et al. designed a bilayer hydrogel actuator with a color-changing fluorescence function to create a hydrogel with a novel function. Green light can activate a fluorescent color-changing switch, causing the inner PBI-HPEI hydrogel layer to unfold and the outer PNIPAM layer to undergo complex deformation [56]. Combining GO-PNIPAM hydrogel layers and TPE-PNIPAM passive hydrogel layers produces sapphire fluorescent hydrogels. Different irradiation positions can yield different 2D/3D shapes (Fig. 4cd) [57]. Fluorescent color-changing hydrogels change color in response to environmental conditions (e.g., temperature, humidity), so they can be applied as temperature/humidity sensors to detect the environment. Additionally, it can be utilised as a fluorescent probe for cell imaging and diagnostics.

Near-infrared light and temperature excited volume changes can be applied in temperature controlled grippers to regulate their grasping behavior along with the encapsulation, capture, and transportation of target objects. In soft robots, the application of bilayer structures with rapid response, diverse deformation, and other distinguishing features holds great promise. To achieve targeted, on demand delivery of biological agents, Fusco et al. developed microsphere-based magnetic sodium alginate packaging (Fig. 4f). Due to the safety of NIR for the human body, magnetic packages that are activated by NIR irradiation can be used to transport drugs [61].

Inspired by the bouncing behavior of human fingers, Hu et al. produced a jumping soft robot based on a rolling carbon nanotube/hydrogel bilayer composite actuator that imitates a gymnast's cartwheel. After being illuminated for 3.56s, the carbon nanotube component released energy that caused the jumping robot to instantly take off and jump up to 32 mm (about five times its own height) [62]. Simulating finger bending by transforming isotropic contraction into anisotropic bending with the rapid dissolution of porous, structured hydrogels [60]. Yang et al. produced a soft robot that can move in a manner resembling that of an inchworm. Composed of two layers of rGO/GO-PDA, the body can bend and deform rapidly in response to light stimulation and return to its original shape upon removal from the light source. Under periodic

**Table 3**  
Photoresponsive hydrogel based on double layer Structure.

Publication	Molecular composition	Energy input	Output	Response time	Application
Zhao et al.(2018)[50]	NFC/PNIPAM-clay	808 nm NIR(6.68 w/cm <sup>2</sup> )	Bending	20s–31s	Actuator Software gripper
Zhang et al.(2014)[52]	GO-PNIPAM NC/ PNIPAM NC	halogen tungsten lamp(with a filter having cut off <600 nm)	Bending	20s–130s	Actuator
Fusco et al.(2014)[61]	NIPAM/PEGDA	785 nm NIR(1.5w/cm <sup>2</sup> )	Rotate/ Bending(3D)	60s–120s	Micro transport robot
Yoon et al.(2016)[54]	PNIPAM-g-MC/PAAM	450–490 nm NIR(41.3 mW/cm <sup>2</sup> )	Bending	30s	Actuator
Peng et al.(2017)[55]	PNIPAM/GO-PNIPAM	halogen tungsten lamp(with a filter having cut off <600 nm)	Bending	60s	Software gripper
Zhao et al.(2017)[51]	GO-PDMAA/PNIPAM	808 nm NIR/(1.25 W/cm <sup>2</sup> )	Bend off	105s	Actuator
Ma et al.(2018)[56]	GO-PNIPAM/PBI-HPEI	532 nm Green light	Bending(2D/3D)	–	Actuator
Gao et al.(2021)[57]	GO-PNIPAM/TPE-PNIPAM	808 nm NIR/365 or 254 nm UV	Bending(2D/3D)	420s(-85°–360°)/ 300s–600s(3D)	Actuator
He et al.(2019)[59]	PolyNIPAM/GO-polyNIPAM	808 nm NIR(2.5 W/cm <sup>2</sup> )	Bending	60s(-189°–200°)	Actuator
Wang et al.(2019)[64]	GO-PDMS/PDMS	980 nm NIR	Swimming	1s–5s(Average 6 nm/s)	Actuator Beluga soft robot
Yang et al.(2019)[63]	rGO/GO-PDA	808 nm NIR(100 mW/cm <sup>2</sup> )	Crawl	1.5s	Inchworm soft robot
Shi et al.(2017)[53]	PNIPAM-AuNPs/ PNIPAM	411 nm Blue light(700mW/cm <sup>2</sup> )	Bending	30s	Actuator

near-infrared light stimulation, it is capable of mimicking the movement of an inchworm by coordinating the advance of its body and feet by 0.6 mm in 1.63s (Fig. 4g) [63]. By dispersing high concentrations of GO in PDMS, Wang et al. designed a beluga soft robot that could swim quickly and was not limited to crawling movements (Fig. 4e). When irradiated with low intensity NIR light, it was able to swim 30 mm in 5s [64]. The degree of deformation of a bilayer structured hydrogel is proportional to the volume change difference between the layers. This difference in volume can be achieved by modifying the composition of the hydrogel to affect the swelling/de-swelling rates of the hydrogel layers. Bilayer structured hydrogels provide additional design and manufacturing choices for actuators due to their quick response time and versatile deformation properties.

#### 4.2. Gradient structure

Gradient structured hydrogels are driven by gradient changes in polymer concentration or cross-linking within the hydrogel to produce swelling differences at different locations [65–67]. In comparison to homogeneous hydrogels, gradient structured mechanicals exhibit recurrence of crosslink density, gradient variation of mechanical and swelling

properties. It is capable of programmable control and can produce anisotropic intelligent responses in response to light stimulation.

Through the slow precipitation of polymers, Luo et al. produced hydrogel actuators with an effective gradient structure. By incorporating polypyrrole nanoparticles, it achieves a dual optical and thermal response. Under the stimulation of a near-infrared laser [68], actions including bending, twisting, and mimicking an octopus swimming were accomplished. Anisotropic hydrogel actuators based on MXene show soft, programmable, and versatile deformation. Hydrogel actuators with a specific network density and structural anisotropy can be created by inducing a concentration gradient of MXene nanosheets on PNIPAM hydrogels through a low electric field. By controlling the low electric field and optical driving (Fig. 5a) [71], various deformation capabilities, such as “U”, “J”, “S”, and “Ω”, can be obtained. The deformation of the shape of hydrogel actuators is caused by the swelling/de-swelling of the cross-linked polymers, and their response rate is typically constrained by the rate of water diffusion. Zhang and his team [133] photopolymerized in situ PNIPAM hydrogels containing MOFs on the surface of PDMS films in order to build fast photoresponsive hydrogel actuators. The porous MOFs are not only excellent photothermal nanosensors, but they also accelerate the adsorption/desorption of water, thereby accelerating the

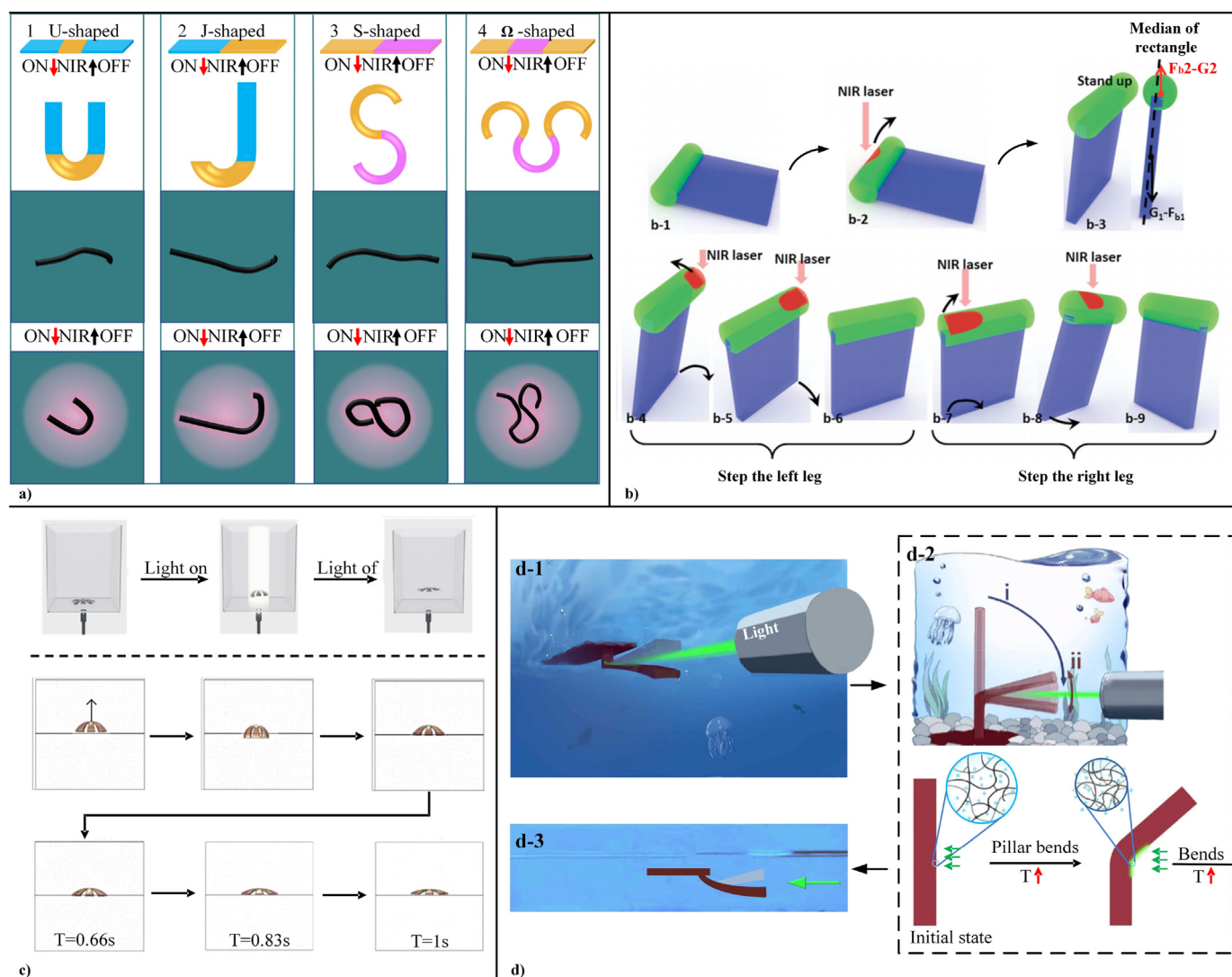


Fig. 5. a) The actuator completes various deformations of “U” “J” “S” and “Ω” [71]. Reproduced with permission. Copyright 2021, Wiley-VCH. b1-b9) CGM actuator walks in near-infrared light [75]. Reproduced with permission. Copyright 2015, Wiley-VCH. c) Jellyfish Software Robot (JSRM) Swatching diagram [76]. Reproduced with permission. Copyright 2021, American Chemical Society. d1-d3) Software Swimming Robot (Oscibot) travel diagram [77]. Reproduced with permission. Copyright 2019, The American Association for the Advancement of Science.



response rate of hydrogel actuators.

Unique structural configurations permit photoresponsive hydrogel actuators to walk, crawl, spin, leap, and swim in a given environment. By employing p(NIPAAm-co-SP-co-AA), Francis et al. built a bipedal hydrogel actuator. One of the polymer structures contains photochromic spiropyran molecules that, when exposed to light in an aqueous environment, contract and deform and travel in a specific direction across the surface of the ratchet [134]. Combining a PA supramolecular polymer with a cross-linked spiropyran network, Li et al. built a bendable and crawling tetrapod hydrogel reptile. By incorporating photosensitive molecules and ferromagnetic nanowires, the ‘Lemon Peel’ soft robot was able to perform a variety of tasks in water [73,74].

Inspired by fish swimming, Wang et al. design a real-time, depth-controllable swimming hydrogel. By adjusting the shape of the hydrogel, the composition of the hydrogel, and the position of the NIR laser, rolling and somersaulting movements were achieved [75]. When the NIR laser strikes the left shoulder of the CGM, the CGM rotates clockwise around the right leg (Fig. 5b–4, b-5). The left shoulder falls to the ground and returns to the tilted position when the NIR laser is removed (Figs. 5b-6). By cycling the NIR light switch, a progressive forward movement of the left and right legs can be accomplished. In order to obtain a swimming robot with controlled swimming speed, Yin and his team designed a jellyfish soft robot (JMSR Fig. 5c) composed of PNIPAM/CNTs. The JMSR's swimming speed (up to 3.37 nm/s) was controlled by adjusting

the concentration of CNTs and the intensity and switching frequency of the incident light [76]. Additionally, the OsciBot (Fig. 5d) is able to generate oscillations and swim away from a light source under the control of a light source drive, enabling reverse phototropism [77]. In the future, these swimming robots could be outfitted with a variety of sensors for observing and exploring biota.

#### 4.3. Oriented structure

Nanoparticles or fibers with an oriented structure are doped into the interior of it to deform the hydrogel and enable actuation [78,79]. The oriented structure of hydrogels is usually obtained in four ways: Utilizing two-dimensional nanosheets to form an oriented structure in the horizontal or vertical direction under the influence of an electric or magnetic field, which is then solidified by in situ polymerization. In order to obtain orientation, the chemical network within the hydrogel is pre-stretched. The coordination of metal ions with the polymer is used to control the flow direction of metal ions in order to create an oriented structure. The ice template method requires the formation of oriented ice crystal structures within the hydrogel in order to obtain the oriented structure of the hydrogel.

Anisotropic hydrogels are currently made up primarily of internally long-range ordered structures and responsive polymers. Anisotropic hydrogels can achieve complex macroscopic orientational movements by

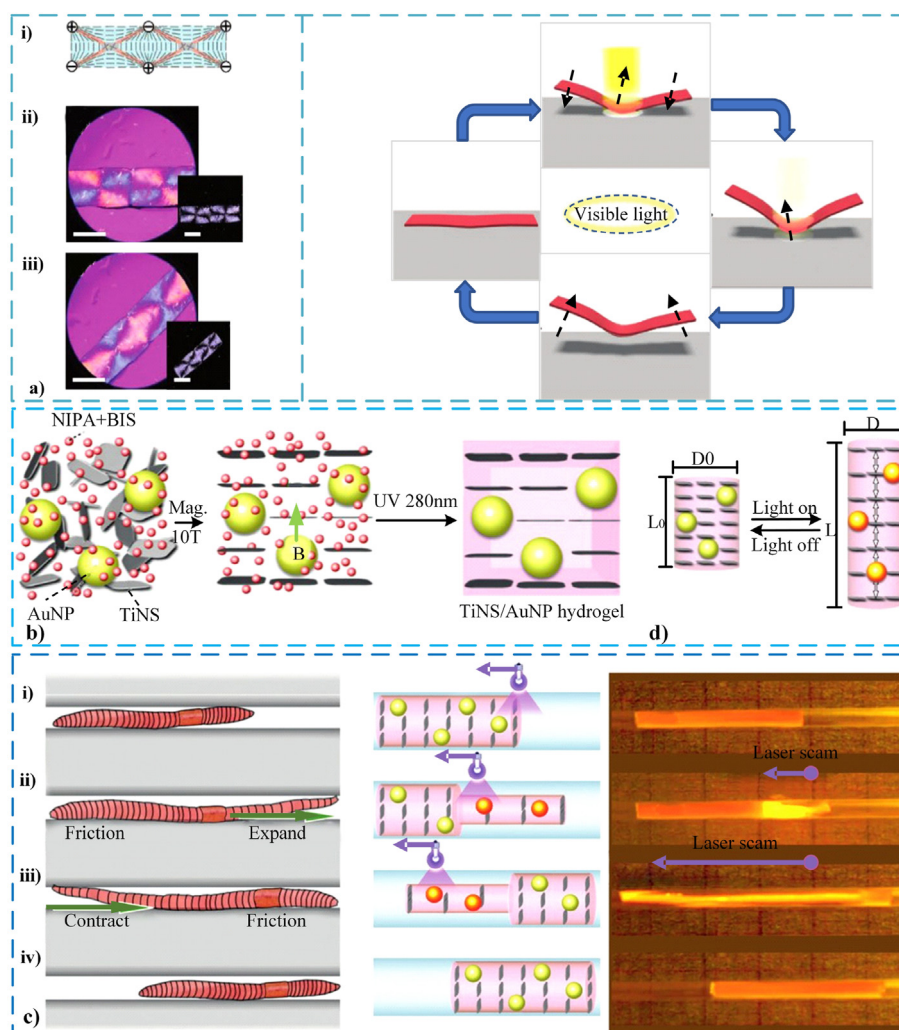


**Fig. 6.** a) Preparation of hydrogel and seagull-like gliding motion [82]. Reproduced with permission. Copyright 2020, Wiley-VCH. b) Tins/AUNP hydrogel preparation and light-induced stretch [81]. c) Light response driver for the bionic earthworm [81]. Reproduced with permission. Copyright 2018, Wiley-VCH.

applying external stimuli based on the synergy of these two forms. By layer-by-layer assembly, gold nanoparticles form oriented structures and are immobilized within the hydrogel, and this anisotropic hydrogel exhibits directional swelling behavior and shape changes when exposed to light. MoS<sub>2</sub>/PNIPAM-co-DMA hydrogel was built by Sun et al [132]. When exposed to near-infrared light, MoS<sub>2</sub> rapidly absorbs heat. There was an inward bending deformation when the temperature exceeded the VPTT of PNIPAM [80]. Sun et al. designed an anisotropic TiNS/AuNR hydrogel to imitate the slithering movement of an earthworm. When a light spot was moved along the axis of a cylinder-shaped gel, it moved in the opposite direction of the laser scan (Fig. 6b and c) [81]. Applying electrodes in the reaction solution, Zhu et al. [82] generated a programmable electric field that caused highly charged nanosheets (NS) to complete their orientation. photoresponsive poly(*N*-isopropylacrylamide) hydrogels were produced by adding gold nanoparticles to the ordered NS. Under light, the resultant ordered hydrogels can be deformed into a variety of three-dimensional shapes (Fig. 6a).

#### 4.4. Patterned structure

Creating patterns in the hydrogel's two-dimensional plane can give the hydrogel anisotropy, allowing for complex deformation and driving [83,84]. Photolithography allows for the design of hydrogel shapes and spatial arrangements. Moreover, it imparts a controlled internal stress to the patterned hydrogel, thereby controlling its deformation. Photolithography is commonly used to create patterned hydrogels due to its controllable and programmable qualities. Ma et al. utilised patterned UV light to reduce GOs in GO-poly(*N*-isopropylacrylamide) (GO-PNIPAM) composite hydrogel sheets before adding a second polymethacrylic acid network to create MA-SPHs from the unreduced GO-PNIPAM hydrogel sheets. It can be driven under remote control by means of light

stimulation. Temperature, pH, and ionic strength can be used to trigger complex deformations in three dimensions [85]. Patterned AuNPs can be embedded in temperature-sensitive hydrogels via two-step photolithography to build deformed hydrogels with Gaussian curvature [88]. Furthermore, half-tone gel lithography requires only two photomasks [87], wherein highly cross-linked dots are embedded in a lightly cross-linked matrix to provide a near-continuous, fully two-dimensional, expanded pattern.

The multi-step electrical orientation and photolithography are able to create three-dimensionally structured anisotropic hydrogels with programmability. Tubular, helical, and curly hydrogels can be made with specific stripe designs (Fig. 7). The muscle-like hydrogel enables controlled crawling, walking, and turning movements by scanning the green light beam at the appropriate direction and rate. This superior motor control is based on both spatiotemporal light stimuli and coordinated frictional dynamic control [86]. The actuators generate asymmetrical frictional forces in response to light stimuli, causing the soft robot to walk and crawl like earthworms and worms. Rehor et al. designed a microscopic (100 μm) hydrogel crawler with photolithography that modulates friction between the body and the substrate. In response to external light stimulation, the thermally responsive poly-*n*-isopropylacrylamide hydrogel containing gold nanoparticles contracts reversibly. Asymmetric friction between the crawler and the substrate is caused by the hydrogel's out of equilibrium collapse and reexpansion. The hydrogel crawler can make tracked, directed movements when combined with eccentric irradiation [89]. The Geca-Robot with stable movement that Wang et al. designed with inspiration from geckos. The muscles of the robot are made up of alternating bands of graphene-PDMS composites and transparent PDMS, while its feet are made up of a variety of triangular PDMS micro-pillars that were photolithographically created. When confronted with varying degrees of slope and roughness,

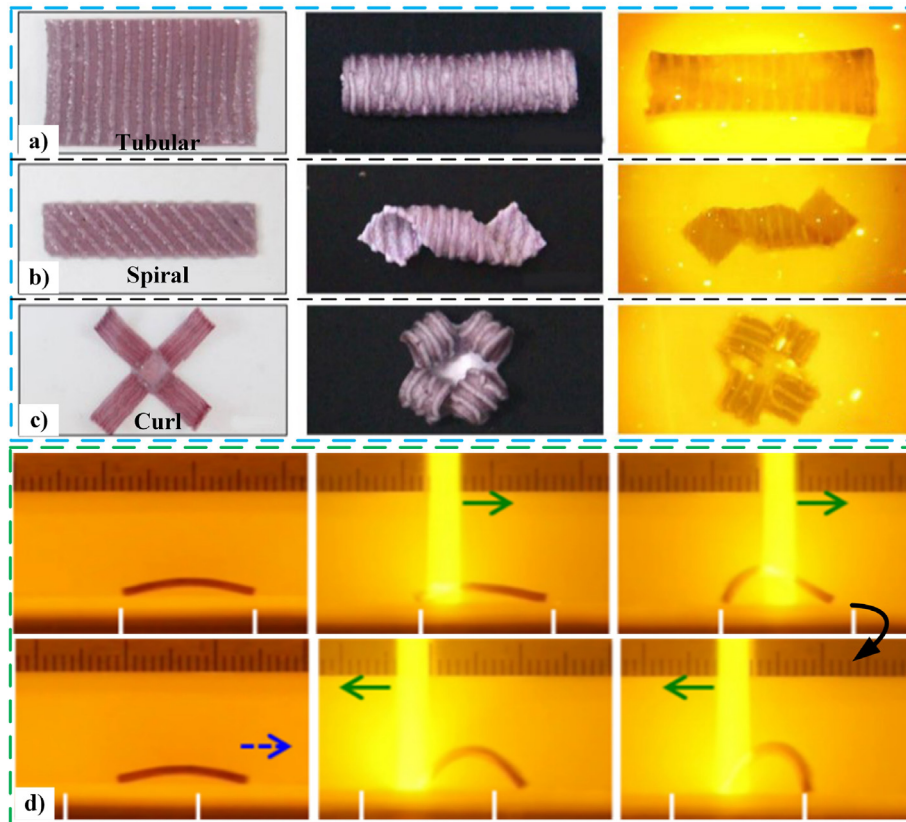


Fig. 7. a-c) Patterned hydrogel deformation under different shapes [86]; a : Tubular , b : Spiral , c : Curl. d) Patterned hydrogel sheet moves in the opposite direction of the scan under repeated light irradiation [86]. Reproduced with permission. Copyright 2020, Springer Nature.

the Geca-Robot can move in a single direction with a caterpillar-like gait and can carry a load roughly 50 times its own size [90].

## 5. Discussion and outlook

### 5.1. Discussion

Photoresponsive hydrogel, a new type of intelligent material, has a promising application in soft robotics. To improve the photoresponsive hydrogel material stability, strength, and response speed, improvements in the material's structure and preparation process are required. As illustrated in Fig. 8, the self-healing properties of mechanical strength, responsiveness, structure, and shape will be discussed separately.

#### 5.1.1. Self healing

Robots are vulnerable to external damage or their own material properties in extreme environments, which can reduce their efficiency. Self-healing capabilities can increase the life and robustness of robots. Photostimulation is non-polluting, controllable, and remotely operable, making it safer and more convenient for soft robot repair. Photoresponsive hydrogels can modulate the binding affinity of the hydrogel to  $\beta$ -CD by photoisomerizing the azobenzene fraction, enabling modification of the crosslink density of the hydrogel. It also self-heals wounds via dynamic host-guest interactions [93–98] and hydrophobic interactions [99]. Reversible complexation of borate esters can also be used to make self-healing hydrogels. Photoresponsive hydrogels based on azobenzene host guest interaction repair can be activated by ultraviolet light and deactivated by visible light [100]. Furthermore, self-healing properties can be obtained by reforming dynamic chemical bonds at damaged sites via hydrogen bonding/metal-ligands [101,102] or by reconstructing networks via hydrogel covalent bonds [103,104]. Table 4 summarizes the properties of photoresponsive hydrogels based on self-healing.

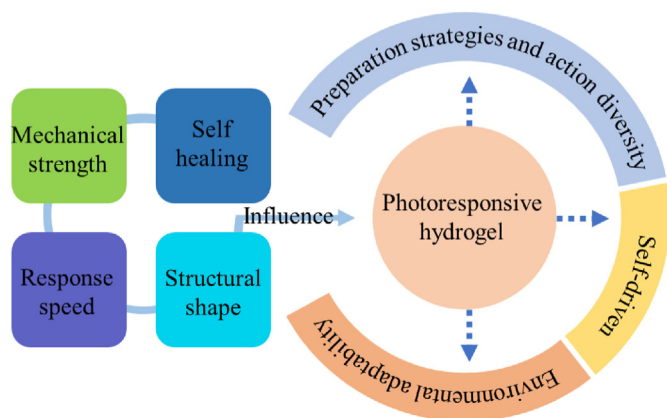


Fig. 8. Discussion and future outlook.

Table 4

The properties of photoresponsive hydrogels based on self-healing.

Publication	Input	Time	Self-healing rate	Method
Xiong et al.(2018)[96]	Vis440nm	2 h	77%	Host-guest interactions
Zhang et al.(2020)[101]	–	20s	96%	Metal–ligand/Hydrogen bonds
Cheng et al.(2019)[103]	NIR980nm	60s	–	Covalent bond reconstruction network
Yang et al.(2017)[100]	UV365 nm/vis 450 nm	–	90%(vis)	Host-guest interactions
Yang et al.(2019)[93]	Dark	24 h	100%	Host-guest interactions
Yu et al.(2018)[104]	UV < 384 nm	NO UV 350min/UV180min	50%/95%	Covalent bond reconstruction network
Wang et al.(2019)[102]	UV	–	–	Hydrogen bonds
Zhang et al.(2020)[99]	NIR3min(60 °C)	–	60%	Hydrophobic interactions
Kim et al.(2020)[97]	UV365nm/Vis430nm	12 h	81.59%	Host-guest interactions
Zheng et al.(2017)[98]	UV365nm/Vis430nm	20min	89.80%	Host-guest interactions

### 5.1.2. Mechanical strength

As the demand for robots grows, the limitations imposed by the mechanical strength deficiencies of conventional hydrogels become more apparent. Soft robots poor mechanical properties make it difficult to accurately manufacture complex structures and make them prone to functional failures when working in unstructured environments. Some existing approaches to improving the mechanical properties of hydrogel soft robots include dual network structures, host-guest recognition, material enhancement methods, and 3/4D printing preparation techniques.

The covalent bonds of conventional covalently bonded double network hydrogels cannot be reformed when subjected to large mechanical deformations, resulting in irreversible and permanent material damage. Finally, the overall mechanical properties of the hydrogel deteriorate. As a result, hybridised or physical DN [105,106] hydrogels with high mechanical properties can be employed to create hydrogel networks. Furthermore, topologically structured hydrogels [107] improve the microstructural regularity of the hydrogel by modulating the “8”-shaped cross-linked ring structure, thereby improving reversibility and mechanical strength. Physical interactions based on supramolecular linkages, such as ionic bonds, hydrogen bonds [108,109], crystallisation, and hydrophobic interactions [110], are reversible in contrast to covalent bonds. Furthermore, host-guest recognition can improve the hydrogel's mechanical strength alongside its self-healing performance.

The type, concentration, and surface properties of nanofillers may be applied to tune hydrogel properties [111]. As physical crosslinkers and fillers, nanoparticles can relax applied stresses and delay the fracture of the hydrogel [112]. GO can also be added to increase crosslinking density by forming H-bonds with the hydrogel backbone, thereby increasing the elastic modulus of the hydrogel [113,114]. Similar to GO, CNT/CNC/NFC [72] can be added to the hydrogel matrix to increase stiffness while preserving biocompatibility [115,116]. In addition, clay and noble metal nanoparticles (e.g., Au, Ag), which are naturally mechanically robust nanofillers, can significantly enhance the mechanical properties of hydrogel matrices [46,117].

4D printing technology is derived from 3D printing with the addition of a “temporal” dimension, enabling printed material structures to respond to external physical field stimuli. By combining specific composite materials, 3D models of target structures [58] (e.g., dual-network hydrogels) can be rapidly fabricated into solids using 3D/4D printing techniques [119,120,135].

### 5.1.3. Response speed

Fast drive strategies, such as fast starts, jumps, must generate high intensity in a short amount of time. Soft robots based on photoresponsive hydrogels can increase their response speed by altering the ratio of light conversion efficiency to actual mechanical energy transfer efficiency. The expansion and contraction of hydrogels are primarily caused by a network of polymers absorbing and releasing water molecules. Currently, hydrogel network structures (e.g., porous hydrogels, comb-like hydrogels [60], and microsphere composite hydrogels [61]) can be modified to allow water molecules to pass easily into and out of the gel network, to reduce diffusion resistance, or to improve response rate by decreasing the

hydrogel feature size. However, the field still faces significant obstacles, such as material and structural design optimization.

#### 5.1.4. Structure shape

Chemical and physical structures, such as cross-link density, pore size, and pore channels, comprise the structure of hydrogels. These structural parameters will directly influence the mechanical properties, water absorption performance, mechanical stability, etc. of hydrogels. For instance, hydrogels with a high crosslink density have greater strength and stiffness and can withstand large tensile or compressive forces, whereas hydrogels with a low crosslink density are softer and can be utilised in bionic robots. Various preparation techniques can yield hydrogels with distinct structures and forms, such as fibrous, spherical, and sheet-like. These various hydrogel shapes can be used to create soft robots with various forms and functions. Fiberous hydrogels are able to design robotic gloves or skin, while spherical hydrogels may be employed to build miniature pumps and sensors.

To achieve the optimal structure and shape for a particular application scenario, the optimal preparation method (free radical polymerization, ionic gelation, physical cross-linking, etc.) is chosen. Using different crosslinking agents, crosslinking times and temperatures, etc., it is possible to produce hydrogels with varying crosslinking densities, resulting in hydrogels with distinct mechanical properties and shapes. By analysing the applicability and performance of the structure and form of hydrogels, it can improve the motility of soft robots and develop new applications.

#### 5.2. Future outlook

The study of photoresponsive hydrogels has made significant strides in recent years, and future research will focus on diversification, intelligence, and autonomy. This paper provides an outlook on preparation strategy, action diversity, environmental adaptability, and self-drive.

##### 5.2.1. Preparation strategy and action diversity of hydrogel soft robot

Most hydrogel soft robots are currently difficult to control multiple movements at once, have complex preparation processes, and have long stimulus response times. In order to improve the efficacy of hydrogel soft robots for rapid and precise action deformation, preparative strategies are investigated. Combining multifunctional materials with hydrogels to design photoresponsive hydrogel soft robots that can operate in harsh environments. For instance, hydrogels can be combined with functions such as fluorescence or shape memory to create new soft robots with collaborative vision detection capabilities. Additionally, 3D/4D printing technologies can be utilised to obtain anisotropic structures of hydrogels in order to customise the hydrogel's shape and internal structure. Smart materials can also be combined with printing technologies to improve assembly efficiency and precision. In the meantime, novel assembly technologies, including micro and nanotechnologies [136] and self-assembly technologies, are being researched and developed to achieve more efficient and accurate assembly.

##### 5.2.2. Environmental adaptability of hydrogel soft robot

Environmental factors restrict the application of the vast majority of photoresponsive hydrogels to the laboratory setting (light intensity, air, etc.). In order to investigate photoresponsive hydrogels that can operate in air, it is important to tackle obstacles such as their unstable operation in the open air, dehydration, and the difficulty of maintaining mechanical deformation. To prevent water diffusion, it is currently possible to add moisturising and elastic coatings, including wetting agents, but the results are not very satisfactory. In order to obtain photoresponsive hydrogels that perform well and can operate in air, new strategies are required. Additionally, the design of photoresponsive hydrogel skin based on ionic skin enables improved access to external information. This can help improve soft robots environmental adaptability and

autonomous driving strategies. The majority of photoresponsive hydrogels' stimulation sources are NIR and UV, and UV has been extensively studied as a stimulation source. Existing NIR [137] excitation technologies are inefficient and difficult to precisely control despite their advantages in tissue penetration and photodamage. Multiple wavelengths (or natural light) trigger an intelligent synergistic response that still needs to be investigated.

##### 5.2.3. Self driving strategy of hydrogel soft robot

Systematization enables the components of a hydrogel soft robot to cooperate with one another, to execute various commands well without additional intervention, and to be lightweight, flexible, compact, and agile; programmability enables it to have capabilities such as programming and machine learning. Therefore, the study of self-driven strategies requires systematization and programming.

There are two ways to study self-driving soft robots: semi-autonomous (requiring external control) and fully autonomous. The semi-autonomous type requires human intervention to replenish energy and provide subsequent instructions. In comparison, the fully autonomous type is more appealing. A soft robot can make autonomous decisions based on its task or external feedback, interacting with its surroundings to decide where to go or whether to avoid the light. Autonomous control requires both internal and external perception as well as the ability to obtain energy from the outside world in order to make optimal decisions. Future development of photoresponsive hydrogel soft robots will aim to achieve stable autonomous sensing, decision making, and movement with minimal human intervention. This serves as a foundation for future research into clustered photoresponsive hydrogel soft robots. The robots are able to communicate, share information, and collaborate to perform tasks more efficiently.

## 6. Conclusion

This article reviews photoresponsive hydrogels for soft robots. Based on the response principle, they are divided into three categories: photoisomerization, photo(de)crosslinking, and photothermal hydrogels. Their application in soft robots is discussed based on bilayer structures, gradient structures, oriented structures, and patterned structures. Such as soft grippers, crawling robots, walking robots, jumping robots, swimming robots, and bionic robots. In order to achieve the best design solution in various application scenarios, soft robots based on photoresponsive hydrogels need to consider the advantages and disadvantages of various preparation methods and structures. Finally, this paper discusses the issues affecting the application of photoresponsive hydrogels in the field of soft robotics, along with the analysis in terms of material property improvement, manufacturing and assembly technology advancement, light source technology development, and environmental optimization. These issues will be addressed in the future through multidisciplinary research to advance and develop photoresponsive hydrogel technology.

### Declaration of competing interest

The authors declare that they have no known competing financial interests or personal relationships that could have appeared to influence the work reported in this paper.

### Data availability

Data will be made available on request.

### Acknowledgements

This work was supported by the Natural Science Foundation of Heilongjiang Province [Grant No. LH2021E081]; the Fundamental Research

Foundation for Universities of Heilongjiang Province [Grant No. LGYC2018JQ016]; and the Research Launch Foundation for Heilongjiang Province Postdoctoral.

## Abbreviations

NIR	near-infrared
UV	ultraviolet
Vis	visible light
CD	cyclodextrin
Azo	azobenzene
azoAAm	azobenzene acrylamide monomer
P(NIPAM-AM)	Poly( <i>N</i> -isopropylacrylamide-acrylamide)
Sp	spirobenzopyran
McH	protonated merocyanine form
Mc	merocyanine form
PNIPAM	poly( <i>N</i> -isopropylacrylamide)
BP	black phosphorus
GO	graphene oxide
rGO	reduced graphene oxide
LCST	lower critical solution temperature
PAAm	polyacrylamide
PDMS	polydimethylsiloxane
NFC	nanofibrillated cellulose
PMAA	poly(methylacrylic acid)
Au NPs	gold nanoparticles
Ag NPs	silver nanoparticles
HABI	hexaarylbiimidazole
PU	polyurethane
PNIPAM-g-MC	poly( <i>N</i> -isopropylacrylamide)-graft-methylcellulose
NIPAm	<i>N</i> -isopropylacrylamide
MNPs	magnetic nanoparticles
PDMAA	poly( <i>N,N</i> -dimethylacrylamide)
PBI-HPEI	bisimide-functionalized hyperbranched polyethylenimine
NIPAM	<i>N</i> -isopro-pylacrylamide
VPTT	volume phase transition temperature
NIPAAm	poly(isopropylacrylamide)
PDA	polydopamine
PEGDA	poly(ethylene glycol) diacrylate
PDMAA	poly( <i>N,N</i> -dimethylacrylamide)
IPN	interpenetrating network
PAAc	poly(acrylic acid)
IONP	iron oxide nanoparticle
PAANa	poly(sodium acrylate)
p(NIPAAm-co-SP-co-AA)	<i>N</i> -isopropylacrylamide-co-acrylated spiropyran-co-acrylic acid
PNIPAM/CNTs	poly( <i>N</i> -isopro-pylacrylamide)/carbon nanotubes
NPs	nanoparticles
PNIPAM-co-DMA	Poly( <i>N</i> -isopropylacrylamide-co- <i>N,N'</i> -dimethylacrylamide)
TiNSs	titanate(IV)nanosheets
NS	nanosheets
MA-SPHS	macroscopically anisotropic stimuli-responsive polymer hydrogels
DN	double network
CNC	colloidal nanocrystalline cluster
NFC	nanofibrillated cellulose
MNPs	magnetic nanoparticles
HA	hyaluronic acid
Dox	doxorubicin
PAA	polyacrylic acid
Azo-PDMAEMA	poly{6-[(2,6-dimethoxyphenyl)azo-4-(2',6'dimethoxyphenoxy)propyl dimethylaminoethyl methacrylate-random-poly(2-( <i>N,N'</i> -dimethylaminoethyl) methacrylate)

## References

- [1] Y. Liu, H. Du, L. Liu, J. Leng, Shape memory polymers and their composites in aerospace applications: a review, *Smart Mater. Struct.* 23 (2014), 023001, <https://doi.org/10.1088/0964-1726/23/2/023001>.
- [2] G.Z. Lum, Z. Ye, X. Dong, H. Marvi, O. Erin, W. Hu, M. Sitti, Shape-programmable magnetic soft matter, *Proc. Natl. Acad. Sci. U.S.A.* 113 (2016) E6007–E6015, <https://doi.org/10.1073/pnas.1608193113>.
- [3] X. Du, H. Cui, T. Xu, C. Huang, Y. Wang, Q. Zhao, Y. Xu, X. Wu, Reconfiguration, camouflage, and color-shifting for bioinspired adaptive hydrogel-based millirobots, *Adv. Funct. Mater.* 30 (2020), 1909202, <https://doi.org/10.1002/adfm.201909202>.
- [4] Y.Y. Xiao, Z.C. Jiang, Y. Zhao, Liquid crystal poly merased soft robots, *Adv. Intell. Syst.* (2020), <https://doi.org/10.1002/aisy.202000148>.
- [5] C. Lee, M. Kim, Y.J. Kim, N. Hong, S. Ryu, H.J. Kim, S. Kim, Soft robot review, *Int. J. Control Autom. Syst.* 15 (2017) 3–15, <https://doi.org/10.1007/s12555-016-0462-3>.
- [6] M.C. Koetting, J.T. Peters, S.D. Steichen, N.A. Peppas, Stimulus-responsive hydrogels: theory, modern advances, and applications, *Mater. Sci. Eng. R Rep.* 93 (2015) 1–49, <https://doi.org/10.1016/j.mser.2015.04.001>.
- [7] L. Cui, Y. Yao, E. Yim, The effects of surface topography modification on hydrogel properties, *APL Bioeng.* 5 (2021), 031509, <https://doi.org/10.1063/5.0046076>.
- [8] C.M. Whitaker, E.E. Derouin, M.B. O'connor, C.K. Whitaker, J.A. Whitaker, J.J. Snyder, N.R. Kaufmann, A.N. Gilliard, A.K. Reitmayr, Smart hydrogel sensor for detection of organophosphorus chemical warfare nerve agents, *J. Macromol. Sci. Part Pure Appl. Chem.* 54 (2017) 40–46, <https://doi.org/10.1080/10601325.2017.1250313>.
- [9] J. Xing, D. Liu, G. Zhou, Y. Li, P. Wang, K. Hu, N. Gu, M. Ji, Liposomally formulated phospholipid-conjugated novel near-infrared fluorescence probe for particle size effect on cellular uptake and biodistribution in vivo, *Colloids Surf. B Biointerfaces* 161 (2018) 588–596, <https://doi.org/10.1016/j.colsurfb.2017.11.033>.
- [10] J. ter Schiphorst, S. Coleman, J.E. Stumpel, A. Ben Azouz, D. Diamond, A.P.H.J. Schenning, Molecular design of light-responsive hydrogels, for in situ generation of fast and reversible valves for microfluidic applications, *Chem. Mater.* 27 (2015) 5925–5931, <https://doi.org/10.1021/acs.chemmater.5b01860>.
- [11] K.S. Lim, F. Abinzano, P.N. Bernal, A. Albillos Sanchez, P. Atienza-Roca, I.A. Otto, Q.C. Peiffer, M. Matsusaki, T.B.F. Woodfield, J. Malda, R. Levato, One-step photoactivation of a dual-functionalized bioink as cell carrier and cartilage-binding glue for chondral regeneration, *Adv. Healthc. Mater.* 9 (2020), 1901792, <https://doi.org/10.1002/adhm.201901792>.
- [12] H. Banerjee, O.Y.W. Aaron, B.S. Yeow, H. Ren, Fabrication and initial cadaveric trials of Bi-directional soft hydrogel robotic benders aiming for biocompatible robot-tissue interactions, in: 2018 3rd Int. Conf. Adv. Robot. Mechatron. ICARM, IEEE, Singapore, 2018, pp. 630–635, <https://doi.org/10.1109/ICARM.2018.8610717>.
- [13] X. Le, W. Lu, J. Zhang, T. Chen, Recent progress in biomimetic anisotropic hydrogel actuators, *Adv. Sci.* 6 (2019), 1801584, <https://doi.org/10.1002/advs.201801584>.
- [14] M. Hou, R. Yang, L. Zhang, L. Zhang, G. Liu, Z. Xu, Y. Kang, P. Xue, Injectable and natural humic acid/agarose hybrid hydrogel for localized light-driven photothermal ablation and chemotherapy of cancer, *ACS Biomater. Sci. Eng.* 4 (2018) 4266–4277, <https://doi.org/10.1021/acsbiomaterials.8b01147>.
- [15] S. Fusco, H.-W. Huang, K.E. Peyer, C. Peters, M. Haerberli, A. Ulbers, A. Spyrogiani, E. Pellicer, J. Sort, S.E. Pratsinis, B.J. Nelson, M.S. Sakar, S. Pane, Shape-switching microrobots for medical applications: the influence of shape in drug delivery and locomotion, *ACS Appl. Mater. Interfaces* 7 (2015) 6803–6811, <https://doi.org/10.1021/acsami.5b00181>.
- [16] C.F. Guimaraes, R. Ahmed, A.P. Marques, R.L. Reis, U. Demirci, Engineering hydrogel-based biomedical photonics: design, fabrication, and applications, *Adv. Mater.* 33 (2021), 2006582, <https://doi.org/10.1002/adma.202006582>.
- [17] D. Han, C. Farino, C. Yang, T. Scott, D. Browe, W. Choi, J.W. Freeman, H. Lee, Soft robotic manipulation and locomotion with a 3D printed electroactive hydrogel, *ACS Appl. Mater. Interfaces* 10 (2018) 17512–17518, <https://doi.org/10.1021/acsami.8b04250>.
- [18] Y. Lee, W.J. Song, J.-Y. Sun, Hydrogel soft robotics, *Mater. Today Phys.* 15 (2020), 100258, <https://doi.org/10.1016/j.mphys.2020.100258>.
- [19] X. Liu, J. Liu, S. Lin, X. Zhao, Hydrogel machines, *Mater. Today* 36 (2020), <https://doi.org/10.1016/j.mattod.2019.12.026>.
- [20] S.V. Paramonov, V. Lokshin, O.A. Fedorova, Spiropyran, chromene or spirooxazine ligands: insights into mutual relations between complexing and photochromic properties, *J. Photochem. Photobiol. C Photochem. Rev.* 12 (2011) 209–236, <https://doi.org/10.1016/j.jphotochemrev.2011.09.001>.
- [21] H. Yamaguchi, Y. Kobayashi, R. Kobayashi, Y. Takashima, A. Hashidzume, A. Harada, Photoswitchable gel assembly based on molecular recognition, *Nat. Commun.* 3 (2012) 603, <https://doi.org/10.1038/ncomms1617>.
- [22] A. Harada, Y. Takashima, M. Nakahata, Supramolecular polymeric materials via cyclodextrin-guest interactions, *Acc. Chem. Res.* 47 (2014) 2128–2140, <https://doi.org/10.1021/ar500109h>.
- [23] P. Palfy-Muhoray, Printed actuators in a flap, *Nat. Mater.* 8 (2009) 614–615, <https://doi.org/10.1038/nmat2502>.
- [24] S.V. Paramonov, V. Lokshin, H. Helms, O.A. Fedorova, Influence of DNA-binding on the photochromic equilibrium of a chromene derivative, *Photochem. Photobiol. Sci.* 10 (2011) 1279–1282, <https://doi.org/10.1039/c1pp05094j>.

- [25] Z. Wang, C. Valenzuela, J. Wu, Y. Chen, L. Wang, W. Feng, Bioinspired freeze-tolerant soft materials: design, properties, and applications, *Small* 18 (2022), 2201597, <https://doi.org/10.1002/small.202201597>.
- [26] H. Zhou, C. Xue, P. Weis, Y. Suzuki, S. Huang, K. Koynov, G.K. Auernhammer, R. Berger, H.-J. Butt, S. Wu, Photoswitching of glass transition temperatures of azobenzene-containing polymers induces reversible solid-to-liquid transitions, *Nat. Chem.* 9 (2017) 145–151, <https://doi.org/10.1038/nchem.2625>.
- [27] H. Wang, C.N. Zhu, H. Zeng, X. Ji, T. Xie, X. Yan, Z.L. Wu, F. Huang, Reversible ion-conducting switch in a novel single-ion supramolecular hydrogel enabled by photoresponsive host–guest molecular recognition, *Adv. Mater.* 31 (2019), 1807328, <https://doi.org/10.1002/adma.201807328>.
- [28] L. Yang, H. Tang, H. Sun, Progress in photo-responsive polypeptide derived nanoassemblies, *Micromachines* 9 (2018) 296, <https://doi.org/10.3390/mi9060296>.
- [29] Y. Zakrevskyy, M. Richter, S. Zakrevska, N. Lomadze, R. von Klitzing, S. Santer, Light-controlled reversible manipulation of Microgel particle size using azobenzene-containing surfactant, *Adv. Funct. Mater.* 22 (2012) 5000–5009, <https://doi.org/10.1002/adfm.201200617>.
- [30] J. ter Schiphorst, G.G. Melpignano, H.E. Amirabadi, M.H.J.M. Houben, S. Bakker, J.M.J. den Toonder, A.P.H.J. Schenning, Photoresponsive passive micromixers based on spiropyran size-tunable hydrogels, *Macromol. Rapid Commun.* 39 (2018), 1700086, <https://doi.org/10.1002/marc.201700086>.
- [31] T. Satoh, K. Sumaru, T. Takagi, T. Kanamori, Fast-reversible light-driven hydrogels consisting of spirobenzopyran-functionalized poly(N-isopropylacrylamide), *Soft Matter* 7 (2011) 8030, <https://doi.org/10.1039/c1sm05797a>.
- [32] Q. Matthew Zhang, X. Li, M.R. Islam, M. Wei, M.J. Serpe, Light switchable optical materials from azobenzene crosslinked poly(N-isopropylacrylamide)-based microgels, *J. Mater. Chem. C* 2 (2014) 6961–6965, <https://doi.org/10.1039/C4TC00653D>.
- [33] K. Unger, P. Salzmann, C. Masciullo, M. Cecchini, G. Koller, A.M. Coclite, Novel light-responsive biocompatible hydrogels produced by initiated chemical vapor deposition, *ACS Appl. Mater. Interfaces* 9 (2017) 17408–17416, <https://doi.org/10.1021/acsami.7b01527>.
- [34] H. Yao, J. Wang, S. Mi, Photo processing for biomedical hydrogels design and functionality: a review, *Polymers* 10 (2018) 11, <https://doi.org/10.3390/polym10010011>.
- [35] P. Payamyar, B.T. King, H. Christian Öttinger, A. Dieter Schlüter, Two-dimensional polymers: concepts and perspectives, *Chem. Commun.* 52 (2016) 18–34, <https://doi.org/10.1039/C5CC07381B>.
- [36] Z. Liu, Q. Lin, Y. Sun, T. Liu, C. Bao, F. Li, L. Zhu, Spatiotemporally controllable and cytocompatible approach builds 3D cell culture matrix by photo-uncaaged-thiol michael addition reaction, *Adv. Mater.* 26 (2014) 3912–3917, <https://doi.org/10.1002/adma.201306061>.
- [37] C. Yi, J. Sun, D. Zhao, Q. Hu, X. Liu, M. Jiang, Influence of photo-cross-linking on emulsifying performance of the self-assemblies of poly(7-(4-vinylbenzyloxy)-4-methylcoumarin-co-acrylic acid), *Langmuir* 30 (2014) 6669–6677, <https://doi.org/10.1021/la500326u>.
- [38] M. Lunzer, L. Shi, O.G. Andriotis, P. Gruber, M. Markovic, P.J. Thurner, D. Ossipov, R. Liska, A. Ovsianikov, A modular approach to sensitized two-photon patterning of photodegradable hydrogels, *Angew. Chem.* 130 (2018) 15342–15347, <https://doi.org/10.1002/ange.201808908>.
- [39] E.R. Ruskowitz, C.A. DeForest, Photoresponsive biomaterials for targeted drug delivery and 4D cell culture, *Nat. Rev. Mater.* 3 (2018) 1–17, <https://doi.org/10.1038/natrevmats.2017.87>.
- [40] C. Wang, B. Willner, I. Willner, Redox-responsive and light-responsive DNA-based hydrogels and their applications, *React. Funct. Polym.* 166 (2021), 104983, <https://doi.org/10.1016/j.reactfunctpolym.2021.104983>.
- [41] Y. Takashima, S. Hatanaka, M. Otsubo, M. Nakahata, T. Kakuta, A. Hashidzume, H. Yamaguchi, A. Harada, Expansion–contraction of photoresponsive artificial muscle regulated by host–guest interactions, *Nat. Commun.* 3 (2012) 1270, <https://doi.org/10.1038/ncomms2280>.
- [42] E. Lee, D. Kim, H. Kim, J. Yoon, Photothermally driven fast responding photo-actuators fabricated with comb-type hydrogels and magnetite nanoparticles, *Sci. Rep.* 5 (2015), 15124, <https://doi.org/10.1038/srep15124>.
- [43] Y. Zhao, L. Song, Z. Zhang, L. Qu, Stimulus-responsive graphene systems towards actuator applications, *Energy Environ. Sci.* 6 (2013) 3520–3536, <https://doi.org/10.1039/c3ee42812e>.
- [44] Y. Huang, J. Liang, Y. Chen, The application of graphene based materials for actuators, *J. Mater. Chem.* 22 (2012) 3671–3679, <https://doi.org/10.1039/C2JM15536B>.
- [45] P. Chen, Q. Ruan, R. Nasser, H. Zhang, X. Xi, H. Xia, G. Xu, Q. Xie, C. Yi, Z. Sun, H. Shahsavani, W. Zhang, Light-fueled hydrogel actuators with controlled deformation and photocatalytic activity, *Adv. Sci.* 9 (2022), 2204730, <https://doi.org/10.1002/advs.202204730>.
- [46] T. Xu, J. Zhang, Y. Zhu, W. Zhao, C. Pan, H. Ma, L. Zhang, A poly(hydroxyethyl methacrylate)–Ag nanoparticle porous hydrogel for simultaneous *in vivo* prevention of the foreign-body reaction and bacterial infection, *Nanotechnology* 29 (2018), 395101, <https://doi.org/10.1088/1361-6528/aad257>.
- [47] Y. Cao, W. Li, F. Quan, Y. Xia, Z. Xiong, Green-light-driven poly(N-isopropylacrylamide-acrylamide)/Fe<sub>3</sub>O<sub>4</sub> nanocomposite hydrogel actuators, *Front. Mater.* 9 (2022). <https://www.frontiersin.org/articles/10.3389/fmats.2022.827608>. (Accessed 17 January 2023). accessed.
- [48] S.J. Jeon, A.W. Hauser, R.C. Hayward, Shape-morphing materials from stimuli-responsive hydrogel hybrids, *Acc. Chem. Res.* 50 (2017) 161–169, <https://doi.org/10.1021/acs.accounts.6b00570>.
- [49] J. Zheng, P. Xiao, X. Le, W. Lu, P. Théato, C. Ma, B. Du, J. Zhang, Y. Huang, T. Chen, Mimosa inspired bilayer hydrogel actuator functioning in multi-environments, *J. Mater. Chem. C* 6 (2018) 1320–1327, <https://doi.org/10.1039/C7TC04879C>.
- [50] Q. Zhao, Y. Liang, L. Ren, Z. Yu, Z. Zhang, F. Qiu, L. Ren, Design and fabrication of nanofibrillated cellulose-containing bilayer hydrogel actuators with temperature and near infrared laser responses, *J. Mater. Chem. B* 6 (2018) 1260–1271, <https://doi.org/10.1039/C7TB02853A>.
- [51] Q. Zhao, W. Hou, Y. Liang, Z. Zhang, L. Ren, Design and fabrication of bilayer hydrogel system with self-healing and detachment properties achieved by near-infrared irradiation, *Polymers* 9 (2017) 237, <https://doi.org/10.3390/polym9060237>.
- [52] E. Zhang, T. Wang, W. Hong, W. Sun, X. Liu, Z. Tong, Infrared-driving actuation based on bilayer graphene oxide-poly(N-isopropylacrylamide) nanocomposite hydrogels, *J. Mater. Chem. A* 2 (2014), 15633, <https://doi.org/10.1039/C4TA02866J>.
- [53] Q. Shi, H. Xia, P. Li, Y.S. Wang, L. Wang, S.X. Li, G. Wang, C. Lv, L.G. Niu, H.B. Sun, Photothermal surface plasmon resonance and interband transition-enhanced nanocomposite hydrogel actuators with hand-like dynamic manipulation, *Adv. Opt. Mater.* 5 (2017), 1700442, <https://doi.org/10.1002/adom.201700442>.
- [54] D. Kim, H. Kim, E. Lee, K.S. Jin, J. Yoon, Programmable volume phase transition of hydrogels achieved by large thermal hysteresis for static-motion bilayer actuators, *Chem. Mater.* 28 (2016) 8807–8814, <https://doi.org/10.1021/acs.chemmater.6b04608>.
- [55] X. Peng, T. Liu, C. Shang, C. Jiao, H. Wang, Mechanically strong Janus poly(N-isopropylacrylamide)/graphene oxide hydrogels as thermo-responsive soft robots, *Chin. J. Polym. Sci.* 35 (2017) 1268–1275, <https://doi.org/10.1007/s10118-017-1970-1>.
- [56] C. Ma, W. Lu, X. Yang, J. He, X. Le, L. Wang, J. Zhang, M.J. Serpe, Y. Huang, T. Chen, Bioinspired anisotropic hydrogel actuators with on-off switchable and color-tunable fluorescence behaviors, *Adv. Funct. Mater.* 28 (2018), 1704568, <https://doi.org/10.1002/adfm.201704568>.
- [57] Q. Gao, P. Pan, G. Shan, M. Du, Bioinspired stimuli-responsive hydrogel with reversible switching and fluorescence behavior served as light-controlled soft actuators, *Macromol. Mater. Eng.* 306 (2021), 2100379, <https://doi.org/10.1002/mame.202100379>.
- [58] Q. Zhao, Y. Liang, L. Ren, F. Qiu, Z. Zhang, L. Ren, Study on temperature and near-infrared driving characteristics of hydrogel actuator fabricated via molding and 3D printing, *J. Mech. Behav. Biomed. Mater.* 78 (2018) 395–403, <https://doi.org/10.1016/j.jmbm.2017.11.043>.
- [59] X. He, Y. Sun, J. Wu, Y. Wang, F. Chen, P. Fan, M. Zhong, S. Xiao, D. Zhang, J. Yang, J. Zheng, Dual-stimulus bilayer hydrogel actuators with rapid, reversible, bidirectional bending behaviors, *J. Mater. Chem. C* 7 (2019) 4970–4980, <https://doi.org/10.1039/c9tc00180h>.
- [60] E. Wang, M.S. Desai, S.-W. Lee, Light-controlled graphene-elastin composite hydrogel actuators, *Nano Lett.* 13 (2013) 2826–2830, <https://doi.org/10.1021/nl401088b>.
- [61] S. Fusco, M.S. Sakar, S. Kennedy, C. Peters, R. Bottani, F. Starsich, A. Mao, G.A. Sotiropoulos, S. Pané, S.E. Pratsinis, D. Mooney, B.J. Nelson, An integrated microbot platform for on-demand, targeted therapeutic interventions, *Adv. Mater.* 26 (2014) 952–957, <https://doi.org/10.1002/adma.201304098>.
- [62] Y. Hu, J. Liu, L. Chang, L. Yang, A. Xu, K. Qi, P. Lu, G. Wu, W. Chen, Y. Wu, Electrically and sunlight-driven actuator with versatile biomimetic motions based on rolled carbon nanotube bilayer composite, *Adv. Funct. Mater.* 27 (2017), 1704388, <https://doi.org/10.1002/adfm.201704388>.
- [63] Y. Yang, D. Li, Y. Shen, Inchworm-Inspired soft robot with light-actuated locomotion, *IEEE Rob. Autom. Lett.* 4 (2019) 1647–1652, <https://doi.org/10.1109/LRA.2019.2896917>.
- [64] X. Wang, N. Jiao, S. Tung, L. Liu, Photoresponsive graphene composite bilayer actuator for soft robots, *ACS Appl. Mater. Interfaces* 11 (2019) 30290–30299, <https://doi.org/10.1021/acsami.9b09491>.
- [65] Y. Yang, Y. Tan, X. Wang, W. An, S. Xu, W. Liao, Y. Wang, Photothermal nanocomposite hydrogel actuator with electric-field-induced gradient and oriented structure, *ACS Appl. Mater. Interfaces* 10 (2018) 7688–7692, <https://doi.org/10.1021/acsami.7b17907>.
- [66] Y. Yang, F. Tian, X. Wang, P. Xu, W. An, Y. Hu, S. Xu, Biomimetic color-changing hierarchical and gradient hydrogel actuators based on salt-induced microphase separation, *ACS Appl. Mater. Interfaces* 11 (2019) 48428–48436, <https://doi.org/10.1021/acsami.9b17904>.
- [67] F. Gao, Z. Xu, Q. Liang, B. Liu, H. Li, Y. Wu, Y. Zhang, Z. Lin, M. Wu, C. Ruan, W. Liu, Direct 3D printing of high strength biohybrid gradient hydrogel scaffolds for efficient repair of osteochondral defect, *Adv. Funct. Mater.* 28 (2018), 1706644, <https://doi.org/10.1002/adfm.201706644>.
- [68] R. Luo, J. Wu, N.D. Dinh, C.H. Chen, Gradient porous elastic hydrogels with shape-memory property and anisotropic responses for programmable locomotion, *Adv. Funct. Mater.* 25 (2015) 7272–7279, <https://doi.org/10.1002/adfm.201503434>.
- [69] M. Ji, N. Jiang, J. Chang, J. Sun, Near-infrared light-driven, highly efficient bilayer actuators based on polydopamine-modified reduced graphene oxide, *Adv. Funct. Mater.* 24 (2014) 5412–5419, <https://doi.org/10.1002/adfm.201401011>.
- [70] Y.Q. Liu, Z.D. Chen, D.D. Han, J.W. Mao, J.N. Ma, Y.L. Zhang, H.-B. Sun, Bioinspired soft robots based on the moisture-responsive graphene oxide, *Adv. Sci.* 8 (2021), 2002464, <https://doi.org/10.1002/advs.202002464>.
- [71] P. Xue, H.K. Bisoyi, Y. Chen, H. Zeng, J. Yang, X. Yang, P. Lv, X. Zhang, A. Priimagi, L. Wang, X. Xu, Q. Li, Near-infrared light-driven shape-morphing of programmable anisotropic hydrogels enabled by MXene nanosheets, *Angew. Chem. Int. Ed.* 60 (2021) 3390–3396, <https://doi.org/10.1002/anie.202014533>.

- [72] P. Lv, X. Lu, L. Wang, W. Feng, Nanocellulose-based functional materials: from chiral photonics to soft actuator and energy storage, *Adv. Funct. Mater.* 31 (2021), 2104991, <https://doi.org/10.1002/adfm.202104991>.
- [73] C. Li, A. Iscen, H. Sai, K. Sato, N.A. Sather, S.M. Chin, Z. Álvarez, L.C. Palmer, G.C. Schatz, S.I. Stupp, Supramolecular-covalent hybrid polymers for light-activated mechanical actuation, *Nat. Mater.* 19 (2020) 900–909, <https://doi.org/10.1038/s41563-020-0707-7>.
- [74] C. Li, G.C. Lau, H. Yuan, A. Aggarwal, V.L. Dominguez, S. Liu, H. Sai, L.C. Palmer, N.A. Sather, T.J. Pearson, D.E. Freedman, P.K. Amiri, M.O. de la Cruz, S.I. Stupp, Fast and programmable locomotion of hydrogel-metal hybrids under light and magnetic fields, *Sci. Robot.* 5 (2020), eabb9822, <https://doi.org/10.1126/scirobotics.abb9822>.
- [75] L. Wang, Y. Liu, Y. Cheng, X. Cui, H. Lian, Y. Liang, F. Chen, H. Wang, W. Guo, H. Li, M. Zhu, H. Ihara, A bioinspired swimming and walking hydrogel driven by light-controlled local density, *Adv. Sci.* 2 (2015), 1500084, <https://doi.org/10.1002/advs.201500084>.
- [76] C. Yin, F. Wei, S. Fu, Z. Zhai, Z. Ge, L. Yao, M. Jiang, M. Liu, Visible light-driven jellyfish-like miniature swimming soft robot, *ACS Appl. Mater. Interfaces* 13 (2021) 47147–47154, <https://doi.org/10.1021/acsami.1c13975>.
- [77] Y. Zhao, C. Xuan, X. Qian, Y. Alsaid, M. Hua, L. Jin, X. He, Soft phototactic swimmer based on self-sustained hydrogel oscillator, *Sci. Robot.* 4 (2019), <https://doi.org/10.1126/scirobotics.aax7112> eaa7112.
- [78] H. Qin, T. Zhang, N. Li, H.P. Cong, S.H. Yu, Anisotropic and self-healing hydrogels with multi-responsive actuating capability, *Nat. Commun.* 10 (2019) 2202, <https://doi.org/10.1038/s41467-019-10243-8>.
- [79] Y.S. Kim, M. Liu, Y. Ishida, Y. Ebina, M. Osada, T. Sasaki, T. Hikima, M. Takata, T. Aida, Thermoresponsive actuation enabled by permittivity switching in an electrostatically anisotropic hydrogel, *Nat. Mater.* 14 (2015) 1002–1007, <https://doi.org/10.1038/nmat4363>.
- [80] Y. Chen, J. Yang, X. Zhang, Y. Feng, H. Zeng, L. Wang, W. Feng, Light-driven biform soft actuators: design, fabrication, and properties, *Mater. Horiz.* 8 (2021) 728–757, <https://doi.org/10.1039/D0MH01406K>.
- [81] Z. Sun, Y. Yamauchi, F. Araoka, Y.S. Kim, J. Bergueiro, Y. Ishida, Y. Ebina, T. Sasaki, T. Hikima, T. Aida, An anisotropic hydrogel actuator enabling earthworm-like directed peristaltic crawling, *Angew. Chem. Int. Ed.* 57 (2018) 15772–15776, <https://doi.org/10.1002/anie.201810052>.
- [82] Q.L. Zhu, C.F. Dai, D. Wagner, M. Daab, W. Hong, J. Breu, Q. Zheng, Z.L. Wu, Distributed electric field induces orientations of nanosheets to prepare hydrogels with elaborate ordered structures and programmed deformations, *Adv. Mater.* 32 (2020), 2005567, <https://doi.org/10.1002/adma.202005567>.
- [83] H. Thérien-Aubin, Z.L. Wu, Z. Nie, E. Kumacheva, Multiple shape transformations of composite hydrogel sheets, *J. Am. Chem. Soc.* 135 (2013) 4834–4839, <https://doi.org/10.1021/ja400518c>.
- [84] J.C. Athas, C.P. Nguyen, B.C. Zarkat, A. Gargava, Z. Nie, S.R. Raghavan, Enzyme-triggered folding of hydrogels: toward a mimic of the venus flytrap, *ACS Appl. Mater. Interfaces* 8 (2016) 19066–19074, <https://doi.org/10.1021/acsami.6b05024>.
- [85] C. Ma, X. Le, X. Tang, J. He, P. Xiao, J. Zheng, H. Xiao, W. Lu, J. Zhang, Y. Huang, T. Chen, A multiresponsive anisotropic hydrogel with macroscopic 3D complex deformations, *Adv. Funct. Mater.* 26 (2016) 8670–8676, <https://doi.org/10.1002/adfm.201603448>.
- [86] Q.L. Zhu, C. Du, Y. Dai, M. Daab, M. Matejdes, J. Breu, W. Hong, Q. Zheng, Z.L. Wu, Light-steered locomotion of muscle-like hydrogel by self-coordinated shape change and friction modulation, *Nat. Commun.* 11 (2020) 5166, <https://doi.org/10.1038/s41467-020-18801-1>.
- [87] J. Kim, J.A. Hanna, M. Byun, C.D. Santangelo, R.C. Hayward, Designing responsive buckled surfaces by halftone gel lithography, *Science* 335 (2012) 1201–1205, <https://doi.org/10.1126/science.1215309>.
- [88] H. Kim, J. Kang, Y. Zhou, A.S. Kuenstler, Y. Kim, C. Chen, T. Emrick, R.C. Hayward, Light-driven shape morphing, assembly, and motion of nanocomposite gel surfers, *Adv. Mater.* 31 (2019), 1900932, <https://doi.org/10.1002/adma.201900932>.
- [89] I. Rehor, C. Maslen, P.G. Moerman, B.G.P. van Ravensteijn, R. van Alst, J. Groenewold, H.B. Eral, W.K. Kegel, Photoresponsive hydrogel microcrawlers exploit friction hysteresis to crawl by reciprocal actuation, *Soft Robot.* 8 (2021) 10–18, <https://doi.org/10.1089/soro.2019.0169>.
- [90] X. Wang, B. Yang, D. Tan, Q. Li, B. Song, Z.S. Wu, A. del Campo, M. Kappel, Z. Wang, S.N. Gorb, S. Liu, L. Xue, Bioinspired footed soft robot with unidirectional all-terrain mobility, *Mater. Today* 35 (2020) 42–49, <https://doi.org/10.1016/j.mattod.2019.12.028>.
- [91] I.M. Garnica-Palaflox, H.O. Estrella-Monroy, N.A. Vázquez-Torres, M. Álvarez-Camacho, A.E. Castell-Rodríguez, F.M. Sánchez-Arévalo, Influence of multi-walled carbon nanotubes on the physico-chemical and biological responses of chitosan-based hybrid hydrogels, *Carbohydr. Polym.* 236 (2020), 115971, <https://doi.org/10.1016/j.carbpol.2020.115971>.
- [92] M. Yang, Y. Xu, X. Zhang, H.K. Bisoyi, P. Xue, Y. Yang, X. Yang, C. Valenzuela, Y. Chen, L. Wang, W. Feng, Q. Li, Bioinspired phototropic MXene-reinforced soft tubular actuators for omnidirectional light-tracking and adaptive photovoltaics, *Adv. Funct. Mater.* 32 (2022), 2201884, <https://doi.org/10.1002/adfm.202201884>.
- [93] M. Yang, L. Wang, Y. Cheng, K. Ma, X. Wei, P. Jia, Y. Gong, Y. Zhang, J. Yang, J. Zhao, Light- and pH-responsive self-healing hydrogel, *J. Mater. Sci.* 54 (2019) 9983–9994, <https://doi.org/10.1007/s10853-019-03547-z>.
- [94] G. Sinawang, M. Osaki, Y. Takashima, H. Yamaguchi, A. Harada, Biofunctional hydrogels based on host-guest interactions, *Polym. J.* 52 (2020) 839–859, <https://doi.org/10.1038/s41428-020-0352-7>.
- [95] M. Salzano de Luna, V. Marturano, M. Manganelli, C. Santillo, V. Ambrogi, G. Filippone, P. Cerruti, Light-responsive and self-healing behavior of azobenzene-based supramolecular hydrogels, *J. Colloid Interface Sci.* 568 (2020) 16–24, <https://doi.org/10.1016/j.jcis.2020.02.038>.
- [96] C. Xiong, L. Zhang, M. Xie, R. Sun, Photoregulating of stretchability and toughness of a self-healable polymer hydrogel, *Macromol. Rapid Commun.* 39 (2018), 1800018, <https://doi.org/10.1002/marc.201800018>.
- [97] Y. Kim, D. Jeong, V.V. Shinde, Y. Hu, C. Kim, S. Jung, Azobenzene-grafted carboxymethyl cellulose hydrogels with photo-switchable, reduction-responsive and self-healing properties for a controlled drug release system, *Int. J. Biol. Macromol.* 163 (2020) 824–832, <https://doi.org/10.1016/j.jbiomac.2020.07.071>.
- [98] Z. Zheng, J. Hu, H. Wang, J. Huang, Y. Yu, Q. Zhang, Y. Cheng, Dynamic softening or stiffening a supramolecular hydrogel by ultraviolet or near-infrared light, *ACS Appl. Mater. Interfaces* 9 (2017) 24511–24517, <https://doi.org/10.1021/acsami.7b07204>.
- [99] Y. Zhang, Y. Wang, Y. Wen, Q. Zhong, Y. Zhao, Self-healable magnetic structural color hydrogels, *ACS Appl. Mater. Interfaces* 12 (2020) 7486–7493, <https://doi.org/10.1021/acsami.9b22579>.
- [100] Q. Yang, P. Wang, C. Zhao, W. Wang, J. Yang, Q. Liu, Light-Switchable self-healing hydrogel based on host-guest macro-crosslinking, *Macromol. Rapid Commun.* 38 (2017), 1600741, <https://doi.org/10.1002/marc.201600741>.
- [101] S. Zhang, B. Xu, X. Lu, L. Wang, Y. Li, N. Ma, H. Wei, X. Zhang, G. Wang, Readily producing a Silly Putty-like hydrogel with good self-healing, conductive and photothermal conversion properties based on dynamic coordinate bonds and hydrogen bonds, *J. Mater. Chem. C* 8 (2020) 6763–6770, <https://doi.org/10.1039/D0TC00814A>.
- [102] Y. Wang, X. Yu, Y. Li, Y. Zhang, L. Geng, F. Shen, J. Ren, Hydrogelation landscape engineering and a novel strategy to design radically induced healable and stimuli-responsive hydrogels, *ACS Appl. Mater. Interfaces* 11 (2019) 19605–19612, <https://doi.org/10.1021/acsami.9b02592>.
- [103] Y. Cheng, K. Ren, C. Huang, J. Wei, Self-healing graphene oxide-based nanocomposite hydrogels serve as near-infrared light-driven valves, *Sensor. Actuator. B Chem.* 298 (2019), 126908, <https://doi.org/10.1016/j.snb.2019.126908>.
- [104] K. Yu, D. Wang, Q. Wang, Tough and self-healable nanocomposite hydrogels for repeatable water treatment, *Polymers* 10 (2018) 880, <https://doi.org/10.3390/polym10080880>.
- [105] H.J. Zhang, T.L. Sun, A.K. Zhang, Y. Ikura, T. Nakajima, T. Nonoyama, T. Kurokawa, O. Ito, H. Ishitobi, J.P. Gong, Tough physical double-network hydrogels based on amphiphilic triblock copolymers, *Adv. Mater.* 28 (2016) 4884–4890, <https://doi.org/10.1002/adma.201600466>.
- [106] J.P. Gong, Why are double network hydrogels so tough? *Soft Matter* 6 (2010) 2583–2590, <https://doi.org/10.1039/B924290B>.
- [107] T. Karino, M. Shibayama, K. Ito, Slide-ring gel: topological gel with freely movable cross-links, *Phys. B Condens. Matter* 385–386 (2006) 692–696, <https://doi.org/10.1016/j.physb.2006.05.293>.
- [108] X. Li, Y. Zhao, D. Li, G. Zhang, S. Long, H. Wang, Hybrid dual crosslinked polyacrylic acid hydrogels with ultrahigh mechanical strength, toughness and self-healing properties via soaking salt solution, *Polymer* 121 (2017) 55–63, <https://doi.org/10.1016/j.polymer.2017.05.070>.
- [109] N. Wang, Y. Li, Y. Zhang, Y. Liao, W. Liu, High-strength photoresponsive hydrogels enable surface-mediated gene delivery and light-induced reversible cell adhesion/detachment, *Langmuir* 30 (2014) 11823–11832, <https://doi.org/10.1021/la502916j>.
- [110] Z. Tao, H. Fan, J. Huang, T. Sun, T. Kurokawa, J.P. Gong, Fabrication of tough hydrogel composites from photoresponsive polymers to show double-network effect, *ACS Appl. Mater. Interfaces* 11 (2019) 37139–37146, <https://doi.org/10.1021/acsami.9b13746>.
- [111] J. Jang, J. Hong, C. Cha, Effects of precursor composition and mode of crosslinking on mechanical properties of graphene oxide reinforced composite hydrogels, *J. Mech. Behav. Biomed. Mater.* 69 (2017) 282–293, <https://doi.org/10.1016/j.jmbmm.2017.01.025>.
- [112] Y. Hu, Y. Li, D. Wang, W. Zhou, X. Dong, S. Zhou, C. Wang, Z. Yang, Highly flexible polymer-carbon dot-ferric ion nanocomposite hydrogels displaying super stretchability, ultrahigh toughness, good self-recovery and shape memory performance, *Eur. Polym. J.* 95 (2017) 482–490, <https://doi.org/10.1016/j.eurpolymj.2017.08.044>.
- [113] L. Dai, J. Lu, F. Kong, K. Liu, H. Wei, C. Si, Reversible photo-controlled release of bovine serum albumin by azobenzene-containing cellulose nanofibrils-based hydrogel, *Adv. Compos. Hybrid Mater.* 2 (2019) 462–470, <https://doi.org/10.1007/s42114-019-00112-9>.
- [114] X. Yan, J. Yang, F. Chen, L. Zhu, Z. Tang, G. Qin, Q. Chen, G. Chen, Mechanical properties of gelatin/polyacrylamide/graphene oxide nanocomposite double-network hydrogels, *Compos. Sci. Technol.* 163 (2018) 81–88, <https://doi.org/10.1016/j.compscitech.2018.05.011>.
- [115] S.R. Shin, H. Bae, J.M. Cha, J.Y. Mun, Y.C. Chen, H. Tekin, H. Shin, S. Zarabi, M.R. Dokmeci, S. Tang, A. Khademhosseini, Carbon nanotube reinforced hybrid microgels as scaffold materials for cell encapsulation, *ACS Nano* 6 (2012) 362–372, <https://doi.org/10.1021/nl203711s>.
- [116] J. Yang, C.R. Han, J.F. Duan, F. Xu, R.C. Sun, Mechanical and viscoelastic properties of cellulose nanocrystals reinforced poly(ethylene glycol) nanocomposite hydrogels, *ACS Appl. Mater. Interfaces* 5 (2013) 3199–3207, <https://doi.org/10.1021/am400197r>.

- [117] Y. Zheng, A. Zaoui, Mechanical behavior in hydrated Na-montmorillonite clay, *Phys. Stat. Mech. Its Appl.* 505 (2018) 582–590, <https://doi.org/10.1016/j.physa.2018.03.093>.
- [118] D. Xu, Z. Li, L. Li, J. Wang, Insights into the photothermal conversion of 2D MXene nanomaterials: synthesis, mechanism, and applications, *Adv. Funct. Mater.* 30 (2020), 2000712, <https://doi.org/10.1002/adfm.202000712>.
- [119] Y. Cheng, K.H. Chan, X.Q. Wang, T. Ding, T. Li, X. Lu, G.W. Ho, Direct-ink-write 3D printing of hydrogels into biomimetic soft robots, *ACS Nano* 13 (2019) 13176–13184, <https://doi.org/10.1021/acsnano.9b06144>.
- [120] D. Morales, E. Palleau, M.D. Dickey, O.D. Velev, Electro-actuated hydrogel walkers with dual responsive legs, *Soft Matter* 10 (2014) 1337–1348, <https://doi.org/10.1039/C3SM51921J>.
- [121] S. Xue, Y. Wu, J. Wang, M. Guo, D. Liu, W. Lei, Boron nitride nanosheets/PNIPAM hydrogels with improved thermo-responsive performance, *Materials* 11 (2018) 1069, <https://doi.org/10.3390/ma11071069>.
- [122] K. Zhang, K. Xue, X.J. Loh, Thermo-responsive hydrogels: from recent progress to biomedical applications, *Gels* 7 (2021) 77, <https://doi.org/10.3390/gels7030077>.
- [123] L. Tang, L. Wang, X. Yang, Y. Feng, Y. Li, W. Feng, Poly(N-isopropylacrylamide)-based smart hydrogels: design, properties and applications, *Prog. Mater. Sci.* 115 (2021), 100702, <https://doi.org/10.1016/j.pmatsci.2020.100702>.
- [124] J. Shao, C. Ruan, H. Xie, Z. Li, H. Wang, P.K. Chu, X.F. Yu, Black-phosphorus-incorporated hydrogel as a sprayable and biodegradable photothermal platform for postsurgical treatment of cancer, *Adv. Sci.* 5 (2018), 1700848, <https://doi.org/10.1002/advs.201700848>.
- [125] Q. Bian, M. Jin, S. Chen, L. Xu, S. Wang, G. Wang, Visible-light-responsive polymeric multilayers for trapping and release of cargoes via host-guest interactions, *Polym. Chem.* 8 (2017) 5525–5532, <https://doi.org/10.1039/C7PY00946A>.
- [126] T. Satoh, K. Sumaru, T. Takagi, T. Kanamori, Fast-reversible light-driven hydrogels consisting of spiropyrans-functionalized poly(N-isopropylacrylamide), *Soft Matter* 7 (2011) 8030, <https://doi.org/10.1039/c1sm05797a>.
- [127] S. Chen, Q. Bian, P. Wang, X. Zheng, L. Lv, Z. Dang, G. Wang, Photo, pH and redox multi-responsive nanogels for drug delivery and fluorescence cell imaging, *Polym. Chem.* 8 (2017) 6150–6157, <https://doi.org/10.1039/C7PY01424D>.
- [128] Z. Cai, K. Huang, C. Bao, X. Wang, X. Sun, H. Xia, Q. Lin, Y. Yang, L. Zhu, Precise construction of cell-instructive 3D microenvironments by photopatterning a biodegradable hydrogel, *Chem. Mater.* 31 (2019) 4710–4719, <https://doi.org/10.1021/acs.chemmater.9b00706>.
- [129] Q. Yang, P. Wang, C. Zhao, W. Wang, J. Yang, Q. Liu, Light-Switchable self-healing hydrogel based on host-guest macro-crosslinking, *Macromol. Rapid Commun.* 38 (2017), 1600741, <https://doi.org/10.1002/marc.201600741>.
- [130] Y. Cao, W. Li, F. Quan, Y. Xia, Z. Xiong, Green-light-driven poly(N-isopropylacrylamide-acrylamide)/Fe<sub>3</sub>O<sub>4</sub> nanocomposite hydrogel actuators, *Front. Mater.* 9 (2022). <https://www.frontiersin.org/articles/10.3389/fmats.2022.827608>. (Accessed 17 January 2023). accessed.
- [131] E. Lee, D. Kim, H. Kim, J. Yoon, Photothermally driven fast responding photo-actuators fabricated with comb-type hydrogels and magnetite nanoparticles, *Sci. Rep.* 5 (2015), 15124, <https://doi.org/10.1038/srep15124>.
- [132] Z. Lei, W. Zhu, S. Sun, P. Wu, MoS<sub>2</sub>-based dual-responsive flexible anisotropic actuators, *Nanoscale* 8 (2016) 18800–18807, <https://doi.org/10.1039/C6NR07265H>.
- [133] X. Zhang, P. Xue, X. Yang, C. Valenzuela, Y. Chen, P. Lv, Z. Wang, L. Wang, X. Xu, Near-infrared light-driven shape-programmable hydrogel actuators loaded with metal-organic frameworks, *ACS Appl. Mater. Interfaces* 14 (2022) 11834–11841, <https://doi.org/10.1021/acscami.1c24702>.
- [134] W. Francis, A. Dunne, C. Delaney, L. Florea, D. Diamond, Spiropyran based hydrogels actuators—walking in the light, *Sensor. Actuator. B Chem.* 250 (2017) 608–616, <https://doi.org/10.1016/j.snb.2017.05.005>.
- [135] H. Kim, B. Kang, X. Cui, S.-H. Lee, K. Lee, D.-W. Cho, W. Hwang, T.B.F. Woodfield, K.S. Lim, J. Jang, Light-activated decellularized extracellular matrix-based bioinks for volumetric tissue analogs at the centimeter scale, *Adv. Funct. Mater.* 31 (2021), 2011252, <https://doi.org/10.1002/adfm.202011252>.
- [136] Z. Huang, G. Shao, L. Li, Micro/nano functional devices fabricated by additive manufacturing, *Prog. Mater. Sci.* 131 (2023), 101020, <https://doi.org/10.1016/j.pmatsci.2022.101020>.
- [137] J. Yang, X. Zhang, X. Zhang, L. Wang, W. Feng, Q. Li, Beyond the visible: bioinspired infrared adaptive materials, *Adv. Mater.* 33 (2021), 2004754, <https://doi.org/10.1002/adma.202004754>.
- [138] H. Ma, M. Xue, Recent advances in the photothermal applications of two-dimensional nanomaterials: photothermal therapy and beyond, *J. Mater. Chem.* 9 (33) (2021) 17569–17591, <https://doi.org/10.1039/d1ta04134g>.